

Free and Low Cost Datasets for International Mountain Cartography

Martin Gamache

Alpine Mapping Guild

alpinemappingguild@earthlink.net

Abstract:

Analytical relief shading rendered from digital elevation models (DEM) has become a common method to illustrate topography. Effective cartographic displays are achieved when DEMs are combined with landcover information derived from satellite imagery. Until recently, however, finding appropriate DEMs and satellite imagery for mountain cartography in remote international areas was a resource intensive proposition. In the last two years, three new sources of remote sensing imagery have become available free or almost free of costs to mountain cartographers: multispectral imagery and DEMs from the Advanced Spaceborne Thermal Emission and Reflection (ASTER) instrument on board the Terra platform; the Shuttle Radar Topography Mission's (SRTM) C-Band InSAR 3 arc second (~90m) DEMs; and, Earthsat Landsat Geocover mosaics. In addition some service providers have begun offering custom DEMs at various resolutions extracted from Russian topographic maps at reasonable prices. Unfortunately for our purposes some of these datasets are prone to higher failure rates (i.e. data gaps) in high mountain areas with complex terrain, high incidences of cloud cover and/or glaciated landcover.

We discuss the relative merits, limitations and sources of errors associated with these new data sources. We will examine and evaluate proposed and implemented mitigation measures and using actual case studies will demonstrate our methods for fusing these new datasets in order to minimize their limitations.

Keywords: SRTM C-Band; DEM; ASTER; Geocover; data fusion; mountain cartography.

Introduction

Mountain cartography is a resurging discipline that makes use of space collected raster datasets such as satellite imagery and digital elevation models (DEMs)[1]. DEMs are used to model land surfaces and to extract topographic information for 2.5-d visualization, cartographic relief depiction, geomorphological, hydrological and glaciological modeling [1], [2], [3], [4], [5], [6], [7]. In most industrialized countries accurate DEMs have been available for some time and their acquisition from space is not new [8], [9]. What is new is the abundance of affordable and reportedly accurate near-global extent DEMs that have come online in the last two years.

Research in alpine applications not surprisingly, has dominated the initial published results into the use of both ASTER and SRTM DEMs. Glaciologists have welcomed the arrival of the ASTER instrument and have been involved in mission planning to ensure adequate glacier coverage [66]. Quantitative studies analyzing geomorphometric parameters and the accuracy of ASTER derived DEMs have been published and articles describing new applications of these datasets for hydrological, and glaciological modeling are numerous [10], [11], [12], [13], [14], [15], [16], [17], [18], [19], [20], [21], [22], [23], [24], [68]. Published results have also begun to appear for the SRTM quasi-global dataset with the completion of its release during the summer of 2004 [10], [22], [25], [26], [27], [28], [29], [67], [69].

Few investigators have concerned themselves with aesthetic and visualization results obtained from these datasets. Maire and Datcu [30] have described methods for fusing image SPOT with the higher resolution raw X-band SRTM data for virtual reality applications. Cheng & McBean [31] demonstrated the possibilities of ASTER in this regard with a flythrough over Afghanistan for military visualization applications. We hope to take advantage of the work being done in these adjunct fields to provide mountain cartographers with a primer on the potential uses and pitfalls of these new datasets for mountain cartography.

The Alpine Mapping Guild has used these sources of data for cartographic assignments for the American Alpine Club (AAC) and the Norwegian Mountain Touring Club (DNT). Both clubs conduct and report on mountain activities from all over the world and do so on very limited budgets. Recently the AAC has reported on the eastern Himalayas in China and Tibet, the Tien Shan, the Cordillera Huayhuash in Peru and various smaller ranges in Central Asia. The DNT contracted us to provide topographic maps of the Karakol and Tien Shan regions in eastern Kyrgyzstan for its club activities. Our ongoing publishing work in South America also makes use of these data sources. The demands of these projects require aesthetically pleasing and topographically accurate relief presentation. We have been experimenting with the use of unedited SRTM 90m DEMs and relative ASTER ~30m DEMs and have a collection of reference datasets created from Peruvian and Russian topographic maps against which to evaluate them.

Datasets

SRTM DEMs

The Shuttle Radar Topography Mission was a joint venture of NASA's Jet Propulsion Laboratory (JPL), National Imaging & Mapping Agency (NIMA, which has since been renamed the National Geospatial-Intelligence Agency (NGA)) and the German and Italian Space Agencies. The mission collected 12 terabytes of data over 80% of the earth's landmass between 60°N and 56°S in February 2000. 99.96% of the targeted landmass was imaged at least once, 94.595% twice and 50% three times. The DEMs currently distributed by the USGS were derived from interferometric analysis of the C band signal and were processed by NASA. The X band signal and its derived products were processed and are being distributed by the German and Italian Space Agencies. We will be discussing the former.

Rapid changes are taking place in regards to this dataset's distribution and available formats (table 1). SRTM DEMs are now being distributed by several agencies both public and private at three spatial resolutions and at two quality levels:

SRTM 30

This is an update to the well documented GTOPO 30 global digital elevation model. SRTM data were used to enhance and correct the GTOPO30 dataset. 3' SRTM data were averaged to a 10 x 10 cell in order to create a 30 arc second data set [32], GTOPO cells were then replaced with valid SRTM cells. In areas such as the Himalayas where large data voids were prevalent, they remain evident in the 30' data. The data structure and tiling scheme of the GTOPO30 dataset were maintained to ensure consistency between datasets. Height values for the SRTM dataset are referenced to the WGS84 EGM96 geoid and neither datasets were adjusted during the fusing. This dataset is available from the USGS FTP server un-projected in the GTOPO .DEM format or from the University of Maryland Global Land Cover Facility (GLCF) in geoTIFF format as both a global mosaic and by native GTOPO30 tiles. This dataset is useful for small scale maps and are often the only data available to correct data voids in the other datasets discussed below.

3 arc second SRTM

This is the dataset of greatest interest due to its near-global coverage and relatively high resolution (90m at the equator). It is available in both an edited and an unedited format. Unedited data were released on a continent by continent basis and were recently completed with the release of Australian data in July 2004. The data are available from the USGS EROS data server, from the USGS seamless data server, and from the GLCF (table 1). These data are described as being of "research grade", do not meet DTED standards and have not been edited for voids and spurious height values, and water bodies often have a rough appearance. A corrected version of the unedited grade data processed by the Centro Internacional de Agricultura Tropical (CIAT) is also available by special request for parts of the world and will be available through a web interface in fall of 2004 [42].

First generation unedited 3 arc second DEMs are derived from the 1' data by the averaging of 9 elevations samples, and spaced at 3 arc second intervals. Random noise error is thus reduced by

a factor of 3 [32]. Each tile of this dataset contains 1201x 1201 samples and tiles are organized on the DTED model with tile name referring to the longitude and latitude of the south west corner.

The second generation edited DTED format data however are derived by decimation of the 1' data rather than averaging in order to keep matching posts between level 1 and level 2 data [32], [33], [34]. Samples are spaced at 3 arc seconds apart to latitude 50° and 3 arc seconds in latitude and 6 arc seconds apart in longitude between 50° and 60° latitude. Smith and Sandwell [27] consider it likely that the DTED 3' dataset has maintained most of the information in the SRTM data.

Edited data have been quality checked and improved in several ways. Spikes and wells exceeding 100m from surrounding elevations have been removed, oceans have been set to 0 meters, lakes greater than 600m in length have been flattened and set to a constant height. Rivers wider than 183m have been stepped down in height to highlight them, and islands with a major axis exceeding 300m or relief exceeding 15m have been depicted. In addition tile edge pixels have been matched to adjacent pixels to ensure edge matching when they are combined. Voids of 16 continuous pixels or less have been filled by interpolation while large ones have been left. Data are complete for 95% of the coverage area and meet or exceed the 16m vertical and 20m horizontal accuracy requirements (90% confidence). Edited data are available on CDs in both .BIL and DTED format from the USGS EROS data center at a cost of \$45/CD. These data have been grouped into 70 CD regions. They can also be obtained from the new NGA Raster Roam web browser in 4801 x4801 pixel tiles. Unfortunately we were unable to evaluate data from this source due to corrupt files. Boeing and Autometric are currently developing means to correct larger data voids in the data. It is not known at this point if and when the corrected data will be made available to the public [35], [36].

1 arc second SRTM

This dataset provides global coverage but is only publicly available over the continental United States at a comparable resolution to existing USGS DEMs (see Falorni et al. [29] for a detailed comparison). It is thus of limited use for international mountain cartography. Data of comparable resolution from the X-band mission are available from the German Space Agency for a reasonable cost, however, we did not evaluate this dataset as it is more limited in its coverage and is not free.

Source of Errors

Mountainous terrains are particularly prone to three types of error with InSAR systems: layover, shadowing and foreshortening and voids when the slope angle exceeds the incidence angle of the radar beam [10], [34], [37], [38] (see diagram 1). This is of significance for the mountain cartographer as mountain areas typically contain proportionally more steep slopes than other environments. The C band Interferometric Synthetic Aperture Radar (InSAR) instrument used to collect the SRTM data has an incidence angle of between 31° and 61° thus resulting in slopes of corresponding angles being hard to image accurately. Falorni et al. have reported that data void locations show “a bimodal distribution when compared to slope, with a large majority occurring in flat areas and a second peak occurring at high slopes” [29]. We have observed similar error location in our datasets.

Accuracy

The SRTM dataset like many other global datasets has accuracy parameters that describe it globally, while its specific elevation errors are not sufficiently described. A typical dataset scenario as described by Shortridge & Goodchild [39]. In the case of the SRTM data, the 16m stated accuracy specification should be considered as a guideline over terrain with high relief and steep slopes [29]. Rabus et al. have suggested that systematic errors within small regions can occur and in theory should be easy to deal with by adding a single corrective value. As long as the area in question is less than 225 km², SRTM specifications require the data to have variations within ±

6m over this distance [26]. In theory this should be easy to do on a tile by tile basis, however, problems may arise when mosaicing large sections of data. Additionally further investigations into error distribution suggest that elevation variations are neither consistent in their magnitude nor in their distribution but tend to be determined by a combination of topography and shuttle flight path direction, thus the bias may be more difficult to estimate and correct.

Few detailed studies of the accuracy of SRTM data have been published and of those, many are for the X-band component of the mission. Kocak et al. compared both X and C band DEMs to GPS control points, and a DEM created from a 1:25,000 maps over a mountainous area of Turkey. They conclude that most DEM published accuracies including SRTM are unrealistic and only valid over flat, vegetation free areas [10]. Jacobsen has indicated that SRTM DEM accuracy is heterogeneous over the dataset [40].

Toutin has shown that radargrammetric DEM accuracy (which suffers from the same shortcoming as InSAR DEMs in mountains) "is almost linearly correlated with terrain slopes, with larger errors in the strongest slopes" [41]. Falorni et al. compared 1 arc second SRTM data to a 30m USGS DEM. Their results indicated that the vertical error magnitude was strongly correlated to increasing slopes and elevation. Having found both positive and negative errors, they speculate that "the influence of topographic attributes on the sign of errors is due to the side-looking geometry of the sensor. Foreshortening on the slopes facing the sensor and layover on slopes looking away could produce errors with opposite signs that are not completely eliminated during processing of the raw data" [29](see diagram 1). We have observed a similar relationship between the sign of the error and the terrain aspect in three of our study areas.

Over a test site in the Cascades Mountains of the northwestern United States (Tolt River basin, 247 km²) Folarni et al. [29] reported RMSZ errors of 14m, maximum vertical errors of over 100m, horizontal shifts of ~100m, a mean slope error of 4% and data voids over 3% of their study area when comparing SRTM DEMs to USGS DEMs. Jacobsen [40] has reported RMSZ errors of between 3.9m and 13m over various European and North American landscapes while also finding horizontal shifts that may be due to datum conversions. Racoviteanu et al [22] report RMSZ errors of 26m against non glaciated spot points taken from a 1:50,000 topographic map of their mountainous study area in Peru. Jarvis et al [42] compared 3 arc second SRTM data to a DEM derived from a 1:10,000, 10m contour map in Columbia and found elevation differences of up to 112m and mean slope differences of 2.8%. Kocak et al. [10] have reported RMSZ errors of 11.7m over their study area in Turkey. Bolch et al. [23] reported mean differences of ~ 6m over a mountainous region of the Tien Shan when compared to a reference DEM obtained from a Russian 1:100,000, 40m contour map.

Advantages

Despite the shortcomings described above the SRTM dataset has numerous advantages. It provides a more or less homogeneous dataset for 80% of the globe at 10 times greater detail than previously available, this is a significant accomplishment considering the data was collected over 11 days. It may not be ideal for mountain cartography due to shortcomings in the signal properties however over many regions it will be adequate after measures are taken to correct data voids (discussed below). It provides coverage through cloud cover and eliminates problems associated with repeat pass and adjacent orbit systems [8] and in so doing has produced DEMs over segments of the Amazon Basin and the Himalayas that the ASTER instrument has yet to image during a cloud free period. It is in large part free and available unprojected and in standardized non-proprietary formats. It has also been shown that its accuracy surpasses that of all space acquired optical DEMs with resolutions lower than 5m (ASTER, SPOT, Landsat, TK350) [10].

In general, methods for dealing with data failures can be divided into three categories. The first is avoidance; this can be achieved by looking for either alternate data sources or alternate research sites. These can be effective options for those with much flexibility in their work/research objectives but in general the latter is not available to most cartographers and the former would

negate the need for this dataset. We thus focus our attention on the other two approaches, replacement by interpolation and by patching.

Interpolation

Interpolation is defined as the estimation of Z values of a surface at an un-sampled point based on the known Z values of surrounding points [43]. Interpolation appears to be the most common way of dealing with data voids and the method employed so far by most tools that have been implemented for fixing data failures in SRTM (and ASTER) data. The difference lies mostly in the procedure employed for implementing the interpolation and which interpolation scheme is used. It is to be noted that while edited DTED level 1 SRTM data has had data voids of up to 16 contiguous pixels corrected by interpolation, it is not known by which method. Table 2 summarizes some of the interpolation tools designed to fix SRTM data that are currently available. Most GIS packages also provide basic image interpolation tools.

Patching

Patching of error voids using alternate DEM sources is also a common method for dealing with data voids. In a worse case scenario one is faced with the prospect of patching 90m SRTM data with SRTM30 data. There are several tools available for this purpose and they are reviewed in Table 2. In some cases better datasets exist at smaller resolution than the target DEM but at a much improved resolution than SRTM30 (see Nuria example). In the best case scenario an absolute ASTER DEM is available. Patching with relative ASTER may not improve the DEM significantly due to the flaws in the uncorrected ASTER data.

One approach used by CIAT to create a recompiled version of the 3 arc second data involves an ARC INFO routine that generates contour lines from un-patched SRTM data. These contours are then re-interpolated and the resulting DEM is used to patch the gaps in the original data [42], [69]. Some software packages will allow the users to “seed” void areas with good values obtained from patches, scanned paper maps, or GPS data, in order to interpolate from these correct values.

Some comments on patching

Though it may appear counterintuitive it is often necessary to remove more pixels in order to improve SRTM data. Pixels adjacent to data voids are often incorrect; eroding or removing the edge pixels surrounding the voids is often necessary to ensure smooth patching [44], [45].

SRTM DEM data are referenced to the WGS 84 geoid and ASTER data to the WGS Spheroid (absolute DEMs) or are relative. We have found that there can be significant vertical differences due to SRTM aspect related errors and to the relative heights contained in the ASTER data. It may be useful to try to quantify these biases over adjacent “good” data values and adjust the ASTER patch accordingly. Lönnqvist and Törmä, based their adjustment of two relative ASTER DEMs on the regression equation between the SRTM to be corrected and the ASTER DEMs used for the patch. They were successful in reducing their RMSZ errors by a factor of three [67].

Most tools described in Table 2 are still in research and/or offer a very limited choice of options as sources of input data for patching. Of the ones listed the most useful has been the System for Automated Geo-Scientific Analysis (SAGA) developed and distributed by Goettingen University, in Germany.

Most patched areas require smoothing and our results with a focal mean filter [23] indicate this to be a good approach. We have found that a 5 x 5 window applied numerous times with various scaling parameters provides good results and good generalization for small scale map creation. The wavelet toolbox in Matlab has successfully been used to remove DEM noise to better effect than moving average filters [29].

We have used Landsat Geocover mosaic imagery to patch over data voids in a shaded relief of the Tien Shan Range (Karakol example below). Our methodology is case specific and

necessitates an image that can be modified to show relief in a way that matches the shading of the DEM. This can sometimes be done by simply inverting the image and re-coloring using an image editing software such as Photoshop. This approach is only useful if one intended to combine a remote sensing image with a DEM and is more suited for smaller scale maps (<1:500,000). It can also be marred by the presence of clouds on the Landsat Geocover mosaics (figs. 10c & 12b).

ASTER DEMs

Description

The ASTER instrument on board Terra collects 14 bands of data at three resolutions. The nadir and backward looking bands 3N and 3B provide us with a 15m stereo pair of satellite images from which 60 km² wide, 30m, 2500 x 2500 pixel DEMs can be extracted. ASTER imagery is collected between 82° N/S latitudes. As of September 2004 over 1.1 million ASTER images were available from the Earth Observation System Data Gateway (EOSDG) as level 1A uncorrected data or geometrically and atmospherically corrected level 1B for \$55.00/scene. Some free imagery is available over the United States and from the GLCF. DEMs are generated from the band 3 images using off-the-shelf specialized software or acquired/requested from NASA through the EOSDG. Level 1A images are necessary if the user intends to stitch images together prior to DEM generation and are reported to provide better results if using GCPs to generate an absolute DEM [46].

For potential users without access to software capable of generating DEMs, a free on-demand system exists for ordering their creation for specific images. Users can place an order for an absolute DEM if they can provide a minimum of eight ground control points (GCPs) or, a relative DEM without GCPs. At the time of last inquiry (September 2004) DEMs requested in this manner were estimated to take approximately 56 weeks to fill. Once a DEM has been created it is made available to all users through the EOSDG. Figure 1 shows the current ASTER DEM coverage. As of September 7, 2004, 4,870 DEMs had been created, of which 91 (1.8%) were absolute DEMs [47]. Hurtado [48] thoroughly describes the methodology used by the USGS EROS Data Center for creating DEMs using PCI Orthoengine software.

ASTER DEMs are delivered in the HDF-EOS format in 16-bit (for files created prior to 01/22/02) or 32 bit format. This format provides a few advantages such as embedding satellite acquired GCPs and complex metadata containing ephemeris, attitude and atmospheric parameters for use in the correction of level 1A data [49]. Horizontal datum varies from NAD83 for Canada and the US and WGS84 for rest of the world. The HDF format is readable by selected Remote Sensing applications (PCI, ENVI, Imagine, Multispec, IDRISI) and GIS tools. HEG and GEOTIFF4 are free public domain utilities useful for converting HDF format files (both DEMs and imagery) to geoTIFFs and USGS format ASCII DEMs.

Sources of errors

Unfortunately for mountain cartographers, high relief, glaciated mountain terrains present the worst case scenario for DEM generation from ASTER imagery [14]. As an optical sensor the ASTER instrument relies on image quality and cross correlation in order to correctly generate elevation data. Image quality is affected by atmospheric factors (cloud cover, cloud shadows), topographic factors (high relief, terrain cast shadows, invisible steep slopes) and land cover factors (saturated pixels, poor contrast between pixels - i.e. glaciers, lakes - complex landcover patterns) [12], [14], [19], [23], [50]. Toutin, in a mountain landscape reported voids over 10% of his DEM due to these factors. As reported with SRTM DEMs a strong correlation between elevation inaccuracies and voids and steep slopes and rugged relief can also be found in the ASTER DEMs [12]. Kamp et al., report that DEMs generated in mountainous areas have a preferential failure mode on slopes over 35° or aspects between 340° and 140° due to the sensor orientation and to lack of direct solar illumination (in the northern hemisphere)[16]. Käab et al.,

reported that East-West oriented mountain crests were prone to error as the shadowed north facing slopes were not visible by the backward looking sensor at a test site in the Swiss Alps [15].

Optical DEMs are characterized by a “pit and hummock” pattern (figs. 9a & 9d) and are also prone to systematic patterns similar to those found on early USGS DEMs (fig 2). The rugged appearance of the surface is due to mismatched points in the stereo pairs and can be minimized by using a large number of Tie Points. These factors may limit their use to the orthorectification of associated imagery and for use as a surface for draping imagery for 2.5d visualization.

Another source of error may be introduced in the conversion from HDF format to GEOTIFF format using the HEG utility. This utility re-projects data from UTM to a lat/long geographic projection and unfortunately a bug in the software crops the southern and eastern edges of the images limiting its usefulness. An updated version of this utility is due to be released in the fall of 2004.

ASTER imagery can be used to generate both relative (no GCPs) and absolute DEMs (with GCPs); we will examine these separately as their performance and accuracy differ.

Relative DEMs

DEM quality and accuracy are intrinsically tied to the availability of accurate stereo GCPs [12], [49], [51], however the majority of DEMs currently available from NASA are relative (~98%). Predicted and estimated errors for these DEMs are in the range RMSE Z of 12.5m [50], RMSE XYZ of 10 to 30m [49], [50]. However the documentation being distributed by the ASTER teams suggests horizontal shifts of up to 700m [70]. These relative DEMs are likely accurate enough for orthorectifying the source ASTER and other imagery or for investigations/visualizations that do not require absolute elevations or integration with data from other sources [52].

Relative DEMs have been used in two glaciological/geomorphological studies of high altitude arid volcanoes in southern Peru [22] and Northern Chile/Bolivia [16].

In Peru the following observations were made:

- RMSZ was calculated at 55m against GPS points and 42m based on spot elevations obtained from a 1:50,000 topographic map. Maximum elevation differences of + 322m were recorded against the topographic map.
- Horizontal offsets of up to 210m were observed and have been reported as common over study areas with high relief.
- Extreme elevation differences attributed to noise were observed at low elevations in the test site.
- Terracing and horizontal stripping were observed as were more terrain detail, artifacts and “spike” anomalies when compared to SRTM and TOPO derived DEMs.

In Northern Chile the following were reported:

- Image tie-point selection is an important factor in ensuring DEM quality, and operator knowledge of the terrain plays a role in this.
- DEM was generated at 30m resolution but resampled to 15m to take advantage of greater data.
- Above 5500m elevation values were low due to the PCI software methodology and ASTER DEM properties at higher elevations (also see [21]).
- DEM was of sufficient quality to generate 2.5d views, solar radiation maps and a periglacial map from geomorphometric analysis.

Absolute DEMs

These are DEMs generated with GCPs. With four or more GCPs theoretical accuracies of 7 to 30m RMSE xyz and slope accuracies of 5° over measurements distances of 100m to 500m are specified [49],[53]. Table 3 summarizes published accuracy results from various global test sites.

Advantages

The VNIR instruments that capture the images (band 3b and 3n) used in DEM generation allow for near simultaneous image capture. This provides a significant advantage over across-track satellite optical DEM systems such as SPOT or IRS-1 C/D. First, images are captured under identical atmospheric, illumination and radiometric conditions. Secondly, ground parameters are also similar which provides the higher image correlation necessary for DEM generation [48]. The near infrared wavelength of band 3 also provides good contrast over forested areas which have typically been difficult to model [10]. Toutin and Cheng [60] compared DEMs derived from SPOT and ASTER to a USGS DEM over an arid landscape in Utah. They found that under ideal conditions (minimal scene radiometric variation) the better resolution and stereo geometry of SPOT imagery still provided higher accuracy and more details. However, under more difficult terrains where conditions between repeat passes would be likely to change, the ASTER DEMs are likely to be as accurate as SPOT DEMs.

A review of the literature and our experience reveals numerous approaches for minimizing errors and dealing with them in ways that do not further degrade the DEM accuracy.

Pre-processing

Scene selection is likely the easiest first step in mitigating data errors. The current web based scene browsers allows for sorting by cloud coverage and to view 3 different color composites browse images in order to verify adequate scene contrast and the absence of clouds or snow cover. Increased repeat coverage as the Terra mission enters its last year of operation generates more possibilities of finding an adequate image. Unfortunately image acquisition does not guarantee the existence of band three data for the generation of DEMs.

Toutin, has reported an almost 10% increase in accuracy with ASTER level 1A imagery that has been corrected for atmospheric distortions such as banding and stripping using the appended radiometric coefficients [12]. Other investigations into the influence of stripping on DEM accuracy may indicate that such corrections do not significantly influence DEM results [68]. It has been suggested that raw level 1A images (with image correction parameters applied) may permit higher accuracy than level1B that has been geometrically corrected [46].

Cheng & McBean [31] used a function of PCI Orthoengine software to stitch ASTER scenes from the same path prior to DEM creation. This software currently allows stitching up to five adjacent scenes. This ensures that the final DEM is contiguous and minimizes the need for further mosaicing post DEM creation, which can introduce seam lines into the datasets (figure 3). Unfortunately, routines for stitching scenes from adjacent paths are still lacking.

The importance of adequate tie point and ground control point quantity and selection has been stressed by numerous authors [38], [49], [51], [46]. Toutin has shown that 15 GCPs was a good compromise in number and that a greater number would improve model rigorousness when the GCPs were of low accuracy (25-30m), such as those obtained from topographic map, a common scenario in international settings [12]. Weeks has suggested that at least 20 tie points are recommended in mountainous regions [53].

If using the pre-processed DEM obtained from the data pool or requested for processing these options may not be available and mitigation measures will be limited to post processing options.

Post processing

Post processing involves blunder removal, void filling, texture removal (if desired) and DEM smoothing [54]. DEMs obtained from the data pool will have been pre-processed in this way using semi automated methods [48], [49], [53]. The literature regarding automatic interpolation of errors is unclear on the threshold at which filters and interpolation (such as median filter) begin to lose usefulness by degrading elevation accuracies excessively [12],[45]. Automatic interpolation methods are a major factor in elevation error propagation in mountainous terrain and interactive

masking and pixel seeding methods are to be favored for areas larger than 200 pixels [12], [54]. A method involving the conversion of a DEM to a triangular irregular network for editing in a stereo workstation with the epipolar images has been proposed but not tested [54]. If vector datasets such as spot elevations, coastlines, lake polygons and drainage polylines are available DEM accuracy could be substantially improved using such a workflow. This would be especially useful for pre-processed DEMs, which could be georeferenced to the vectors in the same process.

Various DEM filtering methods have been applied to DEMs to remove a variety of processing artifacts. Russel & Ochis [55] describe two methods for removing striping, quilting and edge matching discontinuities. Oimoen [56] described a mean profile algorithm to accomplish similar filtering. Albani and Klinkenberg [57] demonstrate how a line based cross-smoothing algorithm intended to clean up Landsat images could successfully be used to remove systematic noise in DEMs derived from British Columbia TRIM Data. Although we did not test the above methods they are presented here as potential solutions to systematic errors that can be found in ASTER DEMs. Post-processing steps performed on data pool acquired DEMs have been described by Hurtado [48]. These apply to the DEMs available from the EOSDG.

Patching of ASTER DEMs can be done in ways similar to those described for SRTM data. No tools have yet to be specifically designed to combine these datasets easily. Blending modules of the SAGA software have successfully been used to patch holes and seams in two mosaiced ASTER DEMs with 90m SRTM [23]. Honikel [45], [58] has reported success with targeted high pass filtering of InSAR DEMs prior to fusing with an optical DEM which had been filtered with a low pass filter. He worked with ERS-1 InSAR data and a SPOT DEM over a rugged region of Spain. The resulting fused DEM showed remarkable reductions in vertical RMS errors and a reduction in the quantity of blunders. Additionally his methodology worked well with data of differing resolutions. Unfortunately his methodology appears to require access to the raw radar elevation data and it is unlikely the processed SRTM data now available to us would be suitable to this methodology. ASTER scenes have significant overlap and adjacent scenes can sometimes be used to make up for missing data such as is the case in our Cordillera Vilcanota case study (fig. 7). This method however is limited as discrepancies between DEMs that were created at different times can be extreme.

The success of patching and data fusion methods is reliant on having datasets that have been accurately co-registered. Evidence suggests there may be a substantial planimetric shift between SRTM and ASTER imagery and DEMs that need to be resolved prior to combining these datasets [59],[70].

GEOCOVER

The Landsat Earthsat Geocover dataset is comprised of three sets of orthorectified imagery representing three eras of Landsat satellites. The product of interest to us are the free seamless 5° latitude x 6° longitude (12°x12° above 60° latitude), color balanced, orthorectified mosaics generated from Landsat 4/5 and Landsat 7 imagery. The spatial resolution of these images varies between 28.5m for the older set to 14.5m for the pan sharpened Landsat 7 ETM+ dataset. In addition to being free these are available for most of the world (Antarctica is not covered). Mosaics are generated as color composites comprised of bands 7, 4, 2 as RGB and are projected to UTM referenced to the WGS datum. Each mosaic spans one UTM zone wide and has a horizontal accuracy of less than 50m RMSE [64],[65]. The mosaics are delivered in MrSID or GeoTIFF format via the web from two sources, the GLCF and NASA, although the latter has been found to be an unreliable source due a high demand and budgetary constraints [61]. The datasets can also be purchased on DVD and CD.

Despite an extensive search to find cloud free images for the entire globe during their creation, these mosaics are sometimes marred by cloud coverage. These clouds and their shadows can be left in or edited out using an image editor. Other disadvantages when working with these images are that unlike traditional satellite imagery the bands are inaccessible. Image

manipulation and color editing are thus also done using an image editor. We have had some success manipulating these images' color tables in index mode (as described in [62]) and saving the resulting palettes so it can be applied to other mosaics. Since the same color scheme is standardized across the entire dataset, this sort of color conversion lends itself well to automation. Table 5 provides a typical landcover key for the 7, 4, 2 band RGB band combination. We have also employed some image simplifying/generalization filters (Buzz Simplifier in particular) not designed for cartographic generalization but very useful in reducing the level of details in these images when using them on smaller scale maps.

These datasets prove themselves most useful when in need of imagery for medium scale maps under tight time constraints. They do not compare to traditional Landsat imagery in terms of manipulation options or other satellite imagery in terms of image resolution. For users with access to remote sensing software it is useful to note that all the images used in compiling the mosaics are also available as band separated, orthorectified, geoTIFFs from the GLCF. A natural color version of the ETM+ mosaics (Geocover Natural Vue) is also commercially available for \$150/scene.

There are several drawbacks to using satellite imagery as a cartographic base; high noise to information ratio, meteorological interference, unpleasant color anomalies, and relief inversion [62]. These flaws, inherent to satellite imagery are somewhat enhanced in the Geocover mosaics as the color scheme is predetermined, and atmospheric correction more tailored to mountain cartography (i.e. ATCOR) can not be performed. Despite these limitations Geocover mosaics are free, provide consistent global coverage and in some situations with some manipulations have been useful to us when other options such as landcover datasets derived from image classification are unavailable or beyond our clients' budgets.

Russian Topographic DEMs (RTD)

Commercial data provider Eastview Cartographic is a leading provider of DEMs extracted from Russian topographic maps of various scales. On short notice they can deliver DEMs at various resolutions, at prices ranging under \$0.015/km² to over \$3.00/km². For small areas at medium to small scales these prices can be competitive when compared to the cost of acquiring and digitizing necessary topographic maps. In many cases the lack of such maps is a significant obstruction to this process. Eastview, with its Russian partners, has access to an extensive collection of Russian topographic maps. It is particularly useful for DEMs of Asian and Eastern European countries.

DEMs are generated by scanning and georeferencing topographic maps, color separating them and semi-automatically vectorizing the images. Height information from contour lines, spot elevations, and hydrology coverages are then used to build a TIN which is then converted to a digital elevation models. DEMs of two levels of quality are generated depending on the intended use. "Telecom" DEMs only use index contours and major hydrological features in the interpolation process, while "High Precision" DEMs suitable for orthorectifying imagery use all vector topographic features available. Final DEMs are verified by examining profiles for spurious out-of-range elevations and checking the DEM against original spot heights [63]. DEM accuracies are referenced to the original map sources and are summarized in Table 4.

Despite these measures production artifacts such as TIN facets and terracing are sometimes visible on RTDs. These may be due to the absence of adequate contour lines in steep areas. Russian topographic maps portray steep areas and cliffs with a combination of index contours and vertical ridge lines. These features make steep areas difficult to vectorize with the same level of accuracy as areas with complete intermediate contours (figs. 4 & 5).

CASE STUDIES

Cordillera Huayhuash, Peru

This study area is located in the Andes of Peru at approximately 10° South latitude and 77° West longitude. Terrain consists of very deep gorges, steep glaciated alpine peaks and glacial valleys. Elevation ranges from 1264m to 5629 m. A 25m DEM created from 1:25,000 contour lines, hydrology, and spot elevation coverages was available as a reference dataset (Fig. 6a). An unedited 3 arc second SRTM tile (S10W078) was downloaded from the NASA JPL FTP server (Fig 6c). One relative ASTER DEM was available for download from the EOSDG over the study area (Fig 6b). The SRTM data were re-projected to UTM and resampled to 30m and 90m using bicubic interpolation. Both the reference and SRTM DEMs were clipped to match the ASTER DEM.

The ASTER dataset shows a very rugged appearance and has void areas along most valley bottoms likely due to cast shadows from the steep, high canyon walls. When overlaid with our vector hydrology layer the horizontal displacement inherent in the relative ASTER DEMs become very apparent with shifts of 200m in the y and over 700m in the x axis. This strong horizontal shift prevented us from investigating the accuracy of the ASTER data against our reference DEM. It does indicate the limitations of the relative ASTER data without further georeferencing.

The SRTM dataset co-registers well with our reference dataset, as evidenced by the correct registration of the hydrology layer. Void values do not appear in significant numbers. Figures 6d and 6f illustrate the residuals between our reference surface and the SRTM surface. A mean difference of -7m, with maximum error of +209m was calculated. Figure 6e shows our error map overlaid on a shaded relief base. Visually there appears to be a relationship between the terrain aspect and the sign of the residuals although a simple linear regression analysis showed no strong statistical relationship.

Cordillera Vilcanota, Peru

The Vilcanota range is located on the eastern edge of the Andean plateau and is characterized by heavily glaciated, isolated massifs. Our study area is located at approximately 71° W longitude 13°50' S latitude. We had planned to use 3 arc second SRTM data to create some indices and location map for our future topographic work in the area. Since we had already created a 50m DEM we've also investigated the accuracies of the SRTM and ASTER datasets against it where they intersect over the area of the Quelccaya Icecap.

We obtained two relative ASTER DEMs which were georeferenced using scene corner coordinates provided in the metadata and merged using PCI Geomatic's Orthoengine software. Height shifts and seams were visible between the two datasets (figs. 7a, 7b, & 7c) which were generated from imagery taken ~21 months apart. Unedited 3 arc second and SRTM 30 data were also obtained. We used both the SRTM30 (fig. 8c) and the 3 arc second datasets (figs 8a & 8b). A reference 50m DEM created from two 1:100,000 Peruvian IGN topographic maps was used to validate the SRTM and ASTER data.

The merged ASTER data reveal significant flaws inherent to the merging process such as seams and height discrepancies. It is clear to us that imagery to be used in the DEM process should be merged prior to the DEM generation process as described by Cheng & McBean [31]. DEMs created separately have significant height shifts of up to several hundred meters. We did not investigate if scenes from the same path were exempt from these issues. Errors between our reference DEM and the ASTER DEMs (resampled to 50m resolution) were calculated by subtracting the ASTER elevations from the reference elevations. Fig. 7c illustrates a spatial distribution that reflects the merged DEMs. One dataset clearly shows elevation values that are greater and one dataset shows errors that are on the whole lesser. The DEM boundaries are

clearly visible in the error map (fig. 7c). Horizontal shifts were observed between the two datasets but were not quantified.

A similar error analysis was conducted for the SRTM data against our reference DEM. The SRTM dataset has elevations ranging from 316m to 6,301m. Our reference dataset ranges from 1,710m to 6,244m, with elevations values correct to ± 50 m. Our residuals ranged from -416m to +5,680m with a mean error of $\sim +60$ m. Voids appear to be concentrated over lakes and steep areas of the terrain. Strongest errors were found in the pixels surrounding the void areas, evidence of the need to remove these in the editing process. In order to correct these errors an SRTM30 DEM was used to patch areas of no data. Voids were first eroded to remove corrupt adjacent values and filled with SRTM data. The patched areas were then re-interpolated. The entire dataset was filtered numerous times using a scaled 5 x 5 focal mean filter. Since the effects of the filter are cumulative we chose to apply it several times with a strong scaling factor to better control its effects. One of the obvious results of this filter is to generalize the terrain thus making it better suited to smaller scale maps which was our intended use (fig 8d). Figure 8e is a comparison of the Auzangate massif as portrayed by the CIAT patched SRTM DEM and the SRTM30 patched and smoothed SRTM data.

Tash Rabat, At Bashy Range, Kyrgyzstan

The At-Bashy Range is a dry, mostly non-glaciated range running east/west along central Kyrgyzstan's southeastern border with China near Torugart Pass and Chatyr Kul Lake (longitude 75° 16' E and latitude 40°39' N). We are currently compiling a topographic map of the Tash Rabat valley. Elevation values range from 2,520m to 5,072m. A 90m "high precision" DEM created from 1:200,000 topographic data was obtained from Eastview Cartographics (fig. 9f). We also acquired 3 arc second SRTM unedited data (fig. 9e) and a relative ASTER DEM created from a July 2003 image (fig 9d).

The ASTER data was georeferenced using scene corner coordinates obtained from the metadata and used to orthorectify the remaining VNIR image (fig. 9b). The void areas of the SRTM data are not numerous and seem concentrated on the higher and steeper slopes. We used the Adobe Photoshop suite of image editing tools and filters to patch these voids while using the ASTER shaded relief image as a rough patch and reference.

The ASTER DEM shows some of the more typical flaws associated with this dataset (figs. 9a and 9d). Terracing on gentle slopes is visible at item 1, "pit and hummock" texture at 2, data voids due to poor image correlation or perhaps snow cover at 3, and at 4 we see a lake level set too low during the DEM editing process.

By comparing the three datasets (figs 9d, 9e, 9f) we see that the SRTM dataset apart from its obvious data voids shows the greatest level of legible detail absent of noise. The terrain representation is much clearer than even the reference DEM which costs over \$400.00 to purchase. The reference DEM has a somewhat blocky appearance and clearly visible at 5 in fig. 9e are TIN artifacts that would require some further editing.

Our final base onto which we would begin overlaying vector line work is shown in figure 9c. To create the image we combined a desaturated copy of the simulated natural color ASTER VNIR image (bands 2, 1 and 50% (3+1) as RGB) shown in fig. 9b with a generalized version to create a composite image that could be merged with the shaded relief image (fig. 9e). Cast shadows and relief inversion were not too prominent and we were able to use the satellite image to good effect. When the imagery permits it, this method provides a quick way to utilize the color information of the satellite imagery without having to resort to any image classification. Geocover mosaics can be used in the same way as we will see in our next example.

Figure 9g shows the orthorectified ASTER imagery draped over the ASTER DEM. For a quick 2.5d scene this works fairly well; in this case we were careful to hide the defects in the ASTER

image by focusing on a relatively blemish free area. The orthorectified ASTER image needed to be shifted significantly in the horizontal plane in order to fit it to the SRTM data. It may be best to orthorectify this imagery with SRTM data when it is available if one intends to merge the two.

Karakol to Inyl'chek

This region lies from the eastern edge of Lake Issyk Kul to the western edge of the Inyl'chek glacier in Northeastern Kyrgyzstan (centered on 79° longitude and 42° latitude) and comprises elevations ranging from 1,608m to 5,697m. The area is dissected by long glacial valleys that drain into Issyk Kul Lake. In the late fall of 2003 we needed to generate a map to be used as a magazine illustration showing the topography of this area at approximately 1:1.6 million. The same map would also be used to obtain a contract from the magazine's publisher for the creation of two 1:100,000 topographic maps of the area. Since there was no budget for this initial locator map, we needed to balance between two economic objectives; keep costs minimal (i.e. use free data), and produce an attractive map (i.e. secure the contract).

3 arc second SRTM data presented itself as an ideal candidate to use as a base since they had recently been released and were free. ASTER data were ruled out for several reasons; the scenes may not be of sufficiently good quality, and if they were, would be too detailed; the large number of scenes necessary to purchase to cover the 20, 477 km² was cost prohibitive, and free scenes were neither available nor was there enough time to order them through the EOSDG (at that time the waiting period was ~3 months). The SRTM30 (fig 10b) data were too coarse to use on their own but would be useful to patch the 3 arc second DEM. A Landsat Geocover mosaic scene covering the area was also obtained (fig 10c). Six 3 arc second SRTM tiles were mosaiced and re-projected to UTM to match the Geocover mosaic (fig 10a). The SRTM30 was resampled to 90m and used to create a rough patch over the missing areas. We then merged a desaturated, inverted image of the Geocover mosaic with the SRTM data to generate figure 10d. A re-colored and generalized Geocover image was then used to provide landcover information (fig. 10e).

Vall de Núria

Our final example was constructed for this conference's location to compare the SRTM data with a 200m DEM of Catalonia and to attempt repairs with this dataset (fig 11b). Two unedited SRTM tiles were obtained from the NASA FTP server (fig 11a). They were re-projected to UTM Zone 31, ED50 DATUM to match the Catalonian data. SRTM data were patched and combined with a 2000 era Geocover mosaic of 14.5m resolution (figs 12b and 13a). Horizontal shifts of ~200m were observed between the two DEMs. Figure 13b illustrates the spatial distribution of errors with a clear trend of north/north eastern aspects being lower than the reference data and south/south western aspects too high. Errors ranging from -290m to +286m were measured with a mean of -0.1 m. It is interesting to note the low mean error over the larger study area (16,870 km²).

Conclusion

We have examined three new, free datasets and discussed their limitations. Our experience with ASTER DEMs would indicate them to be a poor source of quality terrains for relief portrayal on maps without excessive filtering that will degrade their accuracy and the level of detail supposedly afforded by their higher resolution. Under ideal conditions, such as absence of cloud cover, adequate and accurate GCPs and tie points, good contrast between stereo images, north-south trending ridges, these data sets can meet the specified accuracy and can be a source for contour lines of 30m intervals [11], [60]. It is certainly possible to meet some of these criteria through selective imagery choice, GPS field work, and meticulous GCP/TP selection. The majority of DEMs currently available from the EOSDG however, are relative DEMs that most likely do not meet these conditions. Their use may thus be limited to the orthorectification of the ASTER image bands and for use as surfaces for draping imagery for 2.5d visualization.

SRTM 3 arc second DEMs have significant flaws and data voids over mountainous terrain due to the peculiarities of InSAR remote sensing. In particular both positive and negative systematic elevation shifts seem to occur along opposite terrain aspects and ridge and summit elevations are consistently underestimated. A slope bias tending towards steeper average slopes for flat areas and gentler slopes in steep areas has also been observed. Additional work is necessary to document and quantify these shifts in a more robust quantitative way than we have in this paper.

Where SRTM DEMs do not fail however, they have captured a large amount of terrain detail especially over vegetation free areas. Their quality surpasses that of DEMs created from topographic maps at scales smaller than 1:50,000. In some cases data voids may be significant and the time associated with patching may preclude their use. The fusion of SRTM DEMs with ASTER DEMs has some potential to resolve these issues as discussed by Henkel [45]. The JPL is currently investigating this option. Their initial results confirm reports and our observations of significant horizontal and vertical shifts between the two datasets that will first need to be addressed.

The Geocover dataset is a rich depository of largely cloud free Landsat imagery. We feel the mosaic segment of the collection can be used in certain circumstances to add color and texture to maps in a cost effective way. Although we limited our investigation to the mosaic/color balanced product, the real wealth of this dataset resides in the individual Landsat scenes that are also available. Tools and skills peculiar to remote sensing are necessary to make full use of these and for those not inclined to this type of work the mosaics provide them with a quick and easy opportunity to add imagery data to their maps if used judiciously.

As shown in our Tash Rabat example DEMs extracted from Russian topographic maps may be convenient but the quality of the 90m resolution dataset does not match that of the SRTM data where it is absent of gaps. These maps however remain a useful source of patching material in mountainous areas where SRTM data has significant flaws. It is also the only source of elevation data over Eurasia north of 60°.

References

1. Haberling, C., and L. Hurni, (2002). "Mountain cartography: revival of a classic domain" *ISPRS Journal of Photogrammetry and Remote Sensing* 57(1-2): 134-158.
2. Patterson, T., (1997). "A Desktop Approach to Shaded Relief Production", *Cartographic Perspectives* 36.
3. Etzelmüller, B. and J.R. Sulebak, (2000). "Developments in the use of digital elevation models in periglacial geomorphology and glaciology" *Physische Geographie* 41: 35-58.
4. Bishop, M.P., Bonk, R., Kamp, U. and J.F. Shroder, (2001). "Topographic analysis and modeling for alpine glacier mapping" *Polar Geography*, 25: 182-201.
5. Moore I.D., Grayson R.B. & A.D. Ladson, (1991). "Digital terrain modeling: a review of hydrological, geomorphological and biological applications. *Hydrol. Process.*, 5(1): 3-30.
6. Wilson, J. P. and J. C. Gallant, (2000). "Digital terrain analysis" in: *Terrain analysis - principles and applications*. J. C. Gallant, Ed., John Wiley & Sons, Inc.
7. Sidjak, R.W. & R.D. Wheate, (1999). "Glacier mapping of the Illecillewaet icefield, British Columbia, Canada, using Landsat TM and digital elevation data" *International Journal of Remote Sensing*, 20: 273-284.
8. Toutin, T. (2000) "Elevation modeling from satellite data," in *Encyclopædia of Analytical Chemistry*, R. A. Meyers, Ed. Chichester, U.K.: Wiley, 10: 8543–8572.
9. Al-Roussan, N., and G. Petrie, 1998. "System calibration, geometric accuracy testing and validation of DEM and ortho-image data extracted from SPOT stereo-pairs using commercially available image processing systems", *International Archives of Photogrammetry and Remote Sensing, Stuttgart, Germany, September 7-10*, (Bonn, Germany: German Society for Photogrammetry and Remote Sensing), 32(B4): 8-15.
10. Kocak, G. , Büyüksalih, G. and K. Jacobsen, (2004). "Analysis of Digital Elevation Models Determined by High Resolution Space Images" *IntArchPhRS. Band XXXV, Teil B4. Istanbul, 2004, S:* 636-64.
11. Toutin, T. and P. Cheng, (2001). "DEM generation with ASTER stereo data," *Earth Observ. Mag.*, 10(6): 10–13.
12. Toutin, T., (2002). "Three-dimensional mapping with Aster Stereo data in rugged topography." *IEEE Transactions on Geoscience and Remote Sensing* 4(10).
13. Toutin T., (2003). "DEM Extraction from High Resolution Imagery" *Geospatial Today*, 2(3): 31-36.
14. Käab, A., (2002). "Monitoring high-mountain terrain deformation from repeated air- and spaceborne optical data: examples using digital aerial imagery and ASTER data." *ISPRS Journal of Photogrammetry and Remote Sensing* 57(1-2): 39-52.
15. Käab, A., Huggel, C., Paul, F., Wessels, R., Raup, B., Kieffer, H. & J. Kargel, (2003). "Glacier monitoring from ASTER imagery: accuracy and applications." *EARSeL Proceedings, LIS-SIG Workshop, Berne, March 11-13, 2002:* 43-53.

16. Kamp, U., Bolch, T. & J. Olsenholler, (2003). "DEM generation from ASTER satellite data for geomorphometric analysis of Cerro Sillajhuay, Chile/Bolivia." *Proceedings Annual Meeting Imaging and Geospatial Information Society (ASPRS)*, 5.-9.5.2003, Anchorage, U.S.A., 9 pp. (CD).
17. Khalsa, S. J. S., Dyrgerov, M., Khromova, T., Raup, B. H., and R. G. Barry, (2003). "Space-based mapping of glacier changes using ASTER and GIS tools." *International Geoscience and Remote Sensing Symposium IGARSS'03*, Toulouse, France, July 21 - 25, 2003.
18. Khromova, T.E., Dyrgerov, M.B., and R. G. Barry, (2003). "Late-twentieth century changes in glacier extent in the Ak-shirak Range, Central Asia, determined from historical data and ASTER imagery," *Geoph. Res. Letters*, 30(16).
19. Paul, F., Huggel, C. and A. Kääh, (2004). "Combining satellite multispectral image data and a digital elevation model for mapping debris-covered glaciers." *Remote Sensing of Environment*. 89(4): 510-518.
20. Vignon, F., Arnaud, Y., and G. Kaser, (2003). "Quantification of glacier volume change using topographic and ASTER DEMs." *International Geoscience and Remote Sensing Symposium IGARSS'03*, Toulouse, France, July 21 - 25, 2003.
21. Hirano, A., Welch, R. and H. Lang, (2003). "Mapping from ASTER stereo image data: DEM validation and accuracy assessment." *ISPRS Journal of Photogrammetry and Remote Sensing* 57(5-6): 356-370.
22. Racoviteanu, A. Manley, W., Arnaud, Y., and M. Williams, (2003) "Evaluating Digital Elevation Models for glaciologic applications: An Example from Nevado Coropuna, Peruvian Andes" *Submitted to Global and Planetary Change, Special issue, Proceedings of the Symposium on Mass Balance of Andean Glaciers, Valdivia, March 2003.*
23. Bolch, T., Kamp, U., and J. Olsenholler, (2004). "Using ASTER and SRTM DEMs for Studying Geomorphology and Glaciation in High Mountain Areas." *Proceedings 24th Meeting European Association of Remote Sensing Laboratories (EARSeL)*, 25.-27.5.2004, Dubrovnik, Croatia (In Press).
- 24 Bolch, T., (2004). "Using ASTER And SRTM DEMs for Studying Glaciers and Rock Glaciers in the Northern Tien Shan." *Proceedings Part I of the Conference "Teoreticheskiye i Prikladnyye Problemy geografii na rubeschje Stoletij (Theoretical and applied problems of geography on a boundary of centuries)"*, Almaty/Kasakhstan, 8/9th June 2004, p. 254-258. Accessed on line in September 2004: http://www.geographie.uni-erlangen.de/tbolch/lit/Bolch_almaty04.pdf
25. Rignot, E., Rivera, A., and G. Casassa, (2003). "Contribution of the Patagonia Icefields of South America to sea level rise." *Science* 302(5644): 434-437.
26. Rabus, B., Eineder, M., Roth, A., and R. Bamler, (2003). "The shuttle radar topography mission--a new class of digital elevation models acquired by spaceborne radar." *ISPRS Journal of Photogrammetry and Remote Sensing* 57(4): 241-262.
27. Smith, B., and D. Sandwell (2003). "Accuracy and resolution of shuttle radar topography mission data." *Geophysical Research Letters*, 30(9).

28. Koch, A., and P. Lohmann, (2000). "Quality Assessment and Validation of Digital Surface Models Derived from the Shuttle Radar Topography Mission (SRTM)" *IntArchPhRS* (33), Ergänzungsband, im Druck. Accessed on line in September 2004:
http://www.ipi.uni-hannover.de/html/publikationen/2000/koch/Paper620_Abstract.pdf
29. Falorni, G., V. Teles, E.R. Vivoni, R. L. Bras and K. S. Amarutunga, (2004). "Analysis and characterization of the vertical accuracy of digital elevation models from the Shuttle Radar Topography Mission" *Journal Geophysical research, Earth Surface*, (In Press).
30. Maire, C. and M. Datcu, (2004). "Synergy of image and Digital Elevation Models (DEMs) information for Virtual Reality". Accessed on-line in September 2004:
http://earth.esa.int/rtd/Events/ESAEUSC_2004/Pd55_Maire.pdf
31. Cheng, P. and L. McBean, (2002). "Fly-through data generation of Afghanistan." *Earth Observation Magazine*. Accessed on line in September 2004:
<http://www.eomonline.com/Common/currentissues/Jan02/cheng.htm>
32. SRTM_Topo documentation. Accessed on-line in September 2004:
ftp://edcsgs9.cr.usgs.gov/pub/data/srtm/Documentation/SRTM_Topo.txt
33. Hennig, T.A., Kretsch J.L., Pessagno, C.J., Salamonowicz, P.H., and W.L. Stein. (2001). "The Shuttle Radar Topography Mission." *DEM 2001 Proceedings*, Caroline Y. Westort (ed.). 65-77.
34. Shuttle Radar Topography Mission DTED® Level 1 (3-arc second) documentation, accessed on-line in September 2004:
<http://edcsns17.cr.usgs.gov/srtm/index.html>
35. Boeing Awarded \$4 Million Follow-On Award to Process Radar Data from Space Shuttle Endeavour, (2004). Press release, accessed on-line in September 2004:
http://www10.giscafe.com/nbc/articles/view_article.php?section=CorpNews&articleid=136211
36. Farr, T., (2004). Personal communication, archived on-line:
<http://pub7.bravenet.com/forum/537683448/fetch/415383/>
37. Hanssen R.F., (2001). "Radar Interferometry. Data interpretation and analysis" Kluwer Academic Publishers, Dordrecht, Netherlands.
38. Lillesand, T.M., R. Kiefer, and J.W. Chipman, (2004). *Remote Sensing and Image Interpretation*; John Wiley & Sons.
39. Shortridge A.M., and M.F., Goodchild, (1999). "Communicating uncertainty for global datasets" *Proceedings of International Symposium on Spatial Data Quality*, edited by W. Shi, M.F. Goodchild & P.F. Fisher, Hong Kong, pp. 59-65.
40. Jacobsen, Karsten (no date) "Analysis of digital elevation models based on space information". Accessed on-line in September 2004 at:
http://www.ipi.uni-hannover.de/html/publikationen/2004/paper/Jac_0504_earsel.pdf
41. Toutin T., (2002). "Impact of terrain slope and aspect on radargrammetric DEM Accuracy" *ISPRS Journal of Photogrammetry and Remote Sensing* 57(3): 228-240.
- 42 Jarvis, A., Rubiano, J., and A. Cuero (no date). "Comparison of SRTM derived DEM vs. topographic map derived DEM in the region of Dapa." CIAT. Accessed on-line in September 2004: http://gisweb.ciat.cgiar.org/sig/download/laboratory_gis/srtm_vs_topomap.pdf

43. AGI GIS Dictionary, accessed on-line in September 2004:
<http://www.geo.ed.ac.uk/agidexe/term?100>
44. PCI Geomatica (2003). "OrthoEngine 9 User Guide".
45. Honikel, M. (1999). "Strategies and Methods for the fusion of Digital Elevation Models from Optical and SAR Data" *International Archives of Photogrammetry and remote Sensing* 32(part 7-4-3 W6), Valladolid, Spain.
46. PCI Geomatics (no date). "Extracting a DEM from ASTER Data". Accessed on-line in September 2004 at:
http://www.pcigeomatics.com/support_center/quickguides/how_to_aster_dem.pdf
47. LP DAAC user services, personal communication.
48. Hurtado, J.M., (2002). "Extraction of a digital elevation model from ASTER Level 1A stereo imagery using PCI Geomatica OrthoEngine v.8.2.0." Accessed on-line in September 2004 at:
http://www.gps.caltech.edu/~fisheggs/resource/ASTER_DEM_Procedure.pdf
49. Lang, H. R. and R. Welch (1999). "Algorithm Theoretical Basis Document for Aster Digital Elevation Models." Accessed on-line in September 2004 at:
http://eosps0.gsfc.nasa.gov/eos_homepage/for_scientists/atbd/docs/ASTER/atbd-ast-14.pdf
50. Tokunaga, M. and S. Hara (1996). "DEM Accuracy Derived from ASTER Data." Accessed on-line in September 2004 at:
<http://www.gisdevelopment.net/aars/acrs/1996/ts10/ts100007pf.htm>
51. Hirano, A., R. Welch and H. Lang (2003). "Mapping from ASTER stereo image data: DEM validation and accuracy assessment." *ISPRS Journal of Photogrammetry and Remote Sensing* 57(5-6): 356-370.
52. Welch, R., Jordan, T., Lang, H. and Murakami, H. (1998): ASTER as a source for topographic data in the late 1990's. *IEEE Transactions on Geoscience and Remote Sensing*, 36: 1282-1289.
53. Weeks, P. (2003) Personal communication.
54. Toutin T. (2001) Elevation Modelling from Satellite VIR Data: A Review; *International Journal of Remote Sensing* , Vol. 22, No 6, pp. 1097-1225.
55. Russell, E. and H. Ochis, (no date). "MITIGATION METHODS FOR SYSTEMATIC ERRORS IN USGS DEMS". Accessed on-line in September 2004 at:
http://www.ctmap.com/gis_journal/filtering_wp.pdf
56. Oimoen, M.J., (2000). "An effective filter for removal of production artifacts in U.S. Geological Survey 7.5-minute digital elevation models" *Proceedings of the Fourteenth International Conference on Applied Geologic Remote Sensing*, 06-08 November, Las Vegas, Nevada (Veridian ERIM International, Ann Arbor, Michigan), pp. 311-319.
57. Albani, M. and B. Klinkenberg, (2003). "A Spatial Filter for the Removal of Striping Artifacts in Digital Elevation Models" *Photogrammetric Engineering & Remote Sensing* 69(7): 755-765.
58. Honikel, M. (1998). "Fusion of Optical and radar Digital Elevation Models in the Spatial Frequency Domain." *Proceedings of the 2nd Int. Workshop on retrieval of Bio- and Geophysical Parameters from SAR Data for Land Applications*.

59. Olsenholler J. and T. Farr. Archived on-line at:
<http://pub7.bravenet.com/forum/537683448/fetch/394303/>
<http://pub7.bravenet.com/forum/537683448/fetch/399701>
60. Toutin T., and P. Cheng, (2002). "A Comparison of Automated DEM Extraction Results Using Along-Track ASTER and Across-Track SPOT Stereo Images" *Optical Engineering* , 41(9): 2102-2106.
61. Fletcher, R., (2004), Personal communication.
62. Patterson, T., and N.V. Kelso, (2004). "Hal Shelton Revisited: Designing and Producing Natural-Color Maps with Satellite Land Cover Data" *Cartographic Perspectives* 47:28-55.
63. Esser, K., (2004), Personal communication.
64. USGS, (no date). An Introductory Landsat Tutorial for Users of GeoCover Data. Accessed on-line in September 2004 at:
<https://zulu.ssc.nasa.gov/mrsid/tutorial/Landsat%20Tutorial-V1.html> - 92k
65. Tucker, C.J., Grant, D.M., and J.D. Dykstra, (2004). "NASA's Global Orthorectified Landsat Data Set" *Photogrammetric Engineering and Remote Sensing*, 70(3): 313-322.
66. Raup, B., Kieffer, H., Hare, T., and J. Kargel, (2000). "Generation of Data Acquisition Requests for the ASTER Satellite Instrument for Monitoring a Globally Distributed Target: Glaciers," *IEEE Transactions On Geoscience and Remote Sensing*, 38(2): 1105-1112.
67. Lönnqvist M., and M. Törmä, (2004). "Different implications of a spatial boundary, Jebel Bishri between the Desert and the Sown in Syria". Accessed on line in September 2004 at:
<http://www.isprs.org/istanbul2004/comm3/papers/397.pdf>
68. Goncalves, J.A. and A.M. Oliveira, (2004). "Accuracy analysis of DEMs derived from ASTER imagery". Accessed on-line in September 2004 at:
<http://www.isprs.org/istanbul2004/comm3/papers/261.pdf>
69. Jarvis, A., Rubiano, J., Nelson, A., Farrow, A., and M. Mulligan, (2004). "Practical use of SRTM data in the tropics – Comparisons with digital elevation models generated from cartographic data" (unpublished, internal report).
70. NASA, (last updated 1/6/2003). *ASTER Digital Elevation Model – AST14DEM-Relative* Accessed on-line in September 2004 at:
http://asterweb.jpl.nasa.gov/products/release_DEM_relative.htm#4.%20Version%20History

Table 1. SRTM Data availability as of September 2004

	Coverage				Media			Format				Projection			Pricing				
	North America to 60° N	South America	Eurasia	Africa	Australia	Web	CD	DVD	DTED	TIFF	.BIL	ArcGrid	SRTM .HGT	Grid Float	Unprojected/ Geographic	UTM	Data Organisation	Free	Cost
USGS Eros FTP Server																			
SRTM 30	Y	Y	Y	Y	Y	Y	N	N	N	N	N	N	Y	N	Y	N	40°x60° tile	Y	0\$
Unedited SRTM 3	Y	Y	Y	Y	Y	Y	N	N	N	N	N	N	Y	N	Y	N	1° x 1° tile	Y	0\$
Unedited SRTM 1	US Only	N	N	N	N	Y	N	N	N	N	N	N	Y	N	Y	N	1° x 1° tile	Y	0\$
USGS Eros Data Center																			
Finished Level 1 SRTM 3	Y	Y	Y	Y (INCOMPLETE)	N	ORDER ONLY	Y	N	Y	Y	Y	N	N	N	Y	N	1° x 1° tile by CD Region*	N	\$45/CD + \$5 SH
Finished Level 2 SRTM 1	US Only	N	N	N	N	ORDER ONLY	N	Y	Y	Y	N	N	N	N	Y	N	1° x 1° tile by DVD Region**	N	\$60/DVD + \$5 SH
USGS Seamless Server																			
Unedited*** SRTM 3	Y	Y	N	N	N	Y	Y	Y	N	Y	Y	Y	N	Y	Y	N	1° x 1° tile	Y	\$32/CD + \$50
Unedited*** SRTM 1	Y	N	N	N	N	Y	Y	Y	N	Y	Y	Y	N	Y	Y	N	1° x 1° tile	Y	\$60/CD + \$65
GLCF																			
SRTM 30	Y	Y	Y	Y	Y	Y	N	N	N	N	N	N	N	N	Y	N	GTOPO Tiling or Global Mosaic	Y	0\$
Unedited**** SRTM 3	Y	Y	Y	Y	Y	Y	N	N	N	N	N	N	N	N	Y	Y	1° x 1° tile	Y	0\$
Unedited**** SRTM 1	US Only	N	N	N	N	Y	N	N	N	N	N	N	N	N	Y	Y	or WRS-2 Path/Row	Y	0\$
CIAT																			
Canada incomplete	Canada incomplete	Y	incomplete	N	N	Y	N	N	N	N	N	Y	N	N	Y	N	small areas by special request	Y	0\$

* See Map: <http://edcns17.cr.usgs.gov/srtm/index.html> for DTED format or <http://edcns17.cr.usgs.gov/srtmbil/> for .BIL format.

** See Map: <http://edcns17.cr.usgs.gov/srtm/index.html> for DTED format or <http://edcns17.cr.usgs.gov/srtmbil2/> for .BIL format.

*** Eventually to be supplemented by edited data

**** To be supplemented by edited data in Fall 2004

Table 2. SRTM repair tools

SRTM Intepolation tools	Interpolation Method	Cost	Source	Note
Intrepid Software	minimum curvature algorithm	?	Geolimage Ltd SRTM product	Expensive Australian Software, many types of interpolation
Surge Software	ABOS	Free		Limited use for patching, works on limited formats data must be in point form
SRTM Fill	Progressive infilling	Free	3D Nature	Useful for small holes (up to 4 pixels) , but unless voids are eroded, may propagate erroneous edge values, a version enabled for batch processing is available for \$25
SRGAxis		Free	Tao@WTUSM gistudio@tom.com	small utility, good for single pixel fixing. Can import .bil .dem and .hgt formats
DRG SRTM Void Killer		\$83.70 67.70€	http://www.dgadv.com/dgvk/	Utility software for patching with SRTM30 and interpolating over the patch. Only inputs are .hgt format, can only patch with GTOPO data.
CIAT ARC/INFO AML	Interpolates contours created from DEM	Free	http://gisweb.ciat.cgiar.org/sig/90m_data_tropics.htm	Smooth patching, but does not replace missing data, with real data. Need to re-introduce macro-scale terrain detail from GTOPO
Data Fusion/Patching Software	Interpolation Method	Cost	Source	Note
Cirsten Software			http://www.photogrammetry.ethz.ch/research/cirsten/cirsten_fusion.html	
DRG SRTM Void Killer	Pounded average of absolute difference	\$83.70 67.70€	http://www.dgadv.com/dgvk/	Utility software for patching with SRTM30 and interpolating over the patch. Only inputs are .hgt format, can only patch with GTOPO data.
Blackart V3.99	LSQR Laplacian Coupled Interpolation and Substitution	Free	http://www.terrainmap.com/	Utility for patching with SRTM3030 after re-sampling and interpolating over the patch. Only inputs are .hdf and .hgt format, can only patch withGTOPO or DTED data. Works best for correcting 1°x 1°SRTM ,
Terrain Fingerprints		\$1199		Sophisticated utility software for patching and merging DEMs can import/export a variety of file formats, and perform sophisticated analysis
SAGA	Various	Free	Bolch et al. (forthcoming) http://geosun1.uni-geog.gwdg.de/saga/html/index.php	GIS softwarewith good DEM patching and merging utilities can import/export a variety of file formats, and perform sophisticated analysis

Table 3. Errors reported in absolute ASTER DEMs

Site	# of GCP	GCP Source	CP Source	# CP	Point accuracy (m)	maximum errors	x	RMSE (m) y	z	ASTER DEM Resolution (m)	Total Relief (m)	Size of test area (km ²)	Source
Mt. Fuji Japan	5	1:25,000	1:25,000	51	±5		6	6	±26.3	75	2,100	504	A Hirano et al.
Andes Chile/Bolivia	5	1:50,000	1:50,000	53	±10 ±5		19.5	19.5	±15.8	150	2,200	3,163.5	A Hirano et al.
San Bernardino, USA	12	DGPS	1:24,000	16			18	18	±10.1	75	1,500	506.25	A Hirano et al.
Huntsville, USA	8	DGPS	DGPS 30 m USGS DEM	39 512 239,776	? ? ±1.5		9	9	±7.3 ±11.1 ±14.7	30	300	405	A Hirano et al.
Zonguldak, Turkey	18	1:50,000	1:25,000 GPS	?	?		?	?	±12 ±16	?	?	?	Buyuksalih & Jacobsen, 2004 Kocak et al. 2203
Okanagan Lake Canada	35	1:50,000	25 m DEM		±25-30 x/y 10 z	167* 28 (LE68)* 51 (LE90)*				30	1,795	?	Toutin, 2002
Gruben Switzerland	?	?	25 m DEM		?	~500 m			±60	30	2,200		Kaab A, 2002 Kaab et al., 2002
Cordillera Blanca, Peru	?	SPOT Image	DEM from 1:100,000 topo		±10	58 m							Vignon et al., 2002
Tien Shan Kyrgyzstan/Kazakistan	33	GPS 1:100,000	SRTM DEM			-100 m SE Aspects, Slopes >35°				30	1,300		Bolch et al. (forthcoming)
Drum Mountains, USA	8	GPS	GPS 30 m USGS DEM			±13.8 +155 m -109 m Mean 1.9 m 17 m (LE90) 10 m (LE83)	15.8	10.5	7.9				Toutin & Cheng (2001)

*with post-processing

Table 4. Specified accuracy of DEMS from Russian topographic maps

Resolution	Source map scale	Source map contour interval	Source map Horizontal Accuracy*	Source map Vertical Accuracy	Custom pricing**	Off-the -shelf Tile price/size***
Overview DEM 3 arcsecond (~90 m)	1:500,000		25 m to 100 m	100 m	\$0.015 /km ² \$0.035 /km ²	\$70 / 1° x 1°
Country-wide DEM 3 arcsecond (~90 m)	1: 200,000 to 1:250,000	40 m	10 m to 40 m	40 m	\$0.09 /km ² \$0.12 /km ²	\$300 / 1° x 1°
Regional DEM 2 arcsecond (~50 m)	1:100,000	20 m	5 m to 20 m	20 m	\$0.30/km ² \$0.50/km ²	\$130/ 15' x 15'
Local DEM 30 m	1:10,000 to 1:50,000		0.8 m to 10 m	5 to 10 m	\$1.50/km ² \$2.00/km ²	\$80/ 7.5' x 7.5'

* Varies according to terrain type, see East View Cartographic 2002 for details http://www.cartographic.com/documents/accuracy_standards.pdf

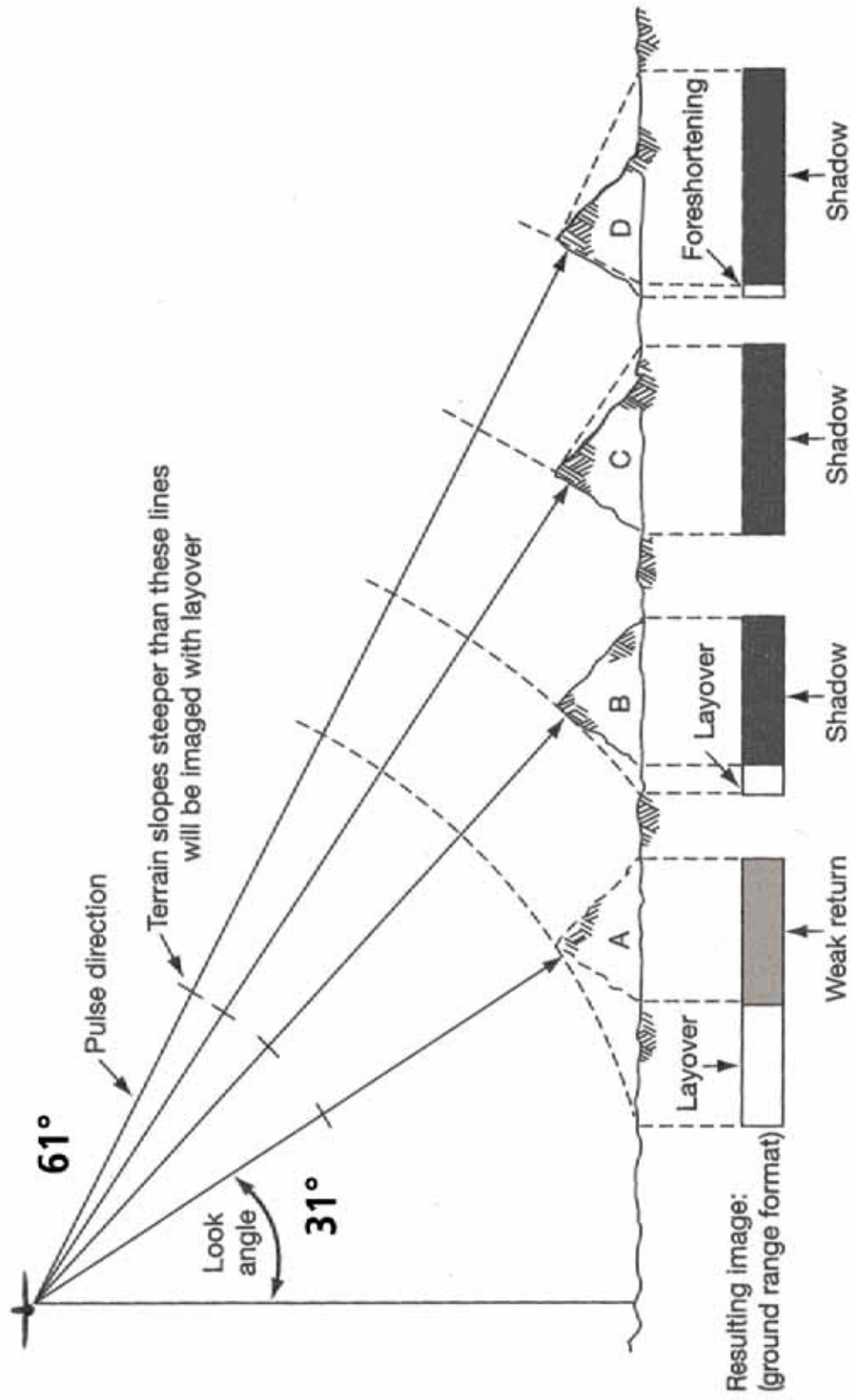
** Lower price is for “telecom” quality Dem.

*** Price includes point and polyline vector data if desired.

Landcover Type	Bands 7,4,2 RGB color appearance
Trees and bushes	Shades of green
Crops	Shades of green
Wetland vegetation	Shades of green
Water	Black to dark blue
Urban areas	Lavender
Bare soil	Lavender
Snow/Ice	Medium blue

Table 5 Geocover mosaic typical landcover key

Diagram 1. SRTM Terrain Relief Displacement



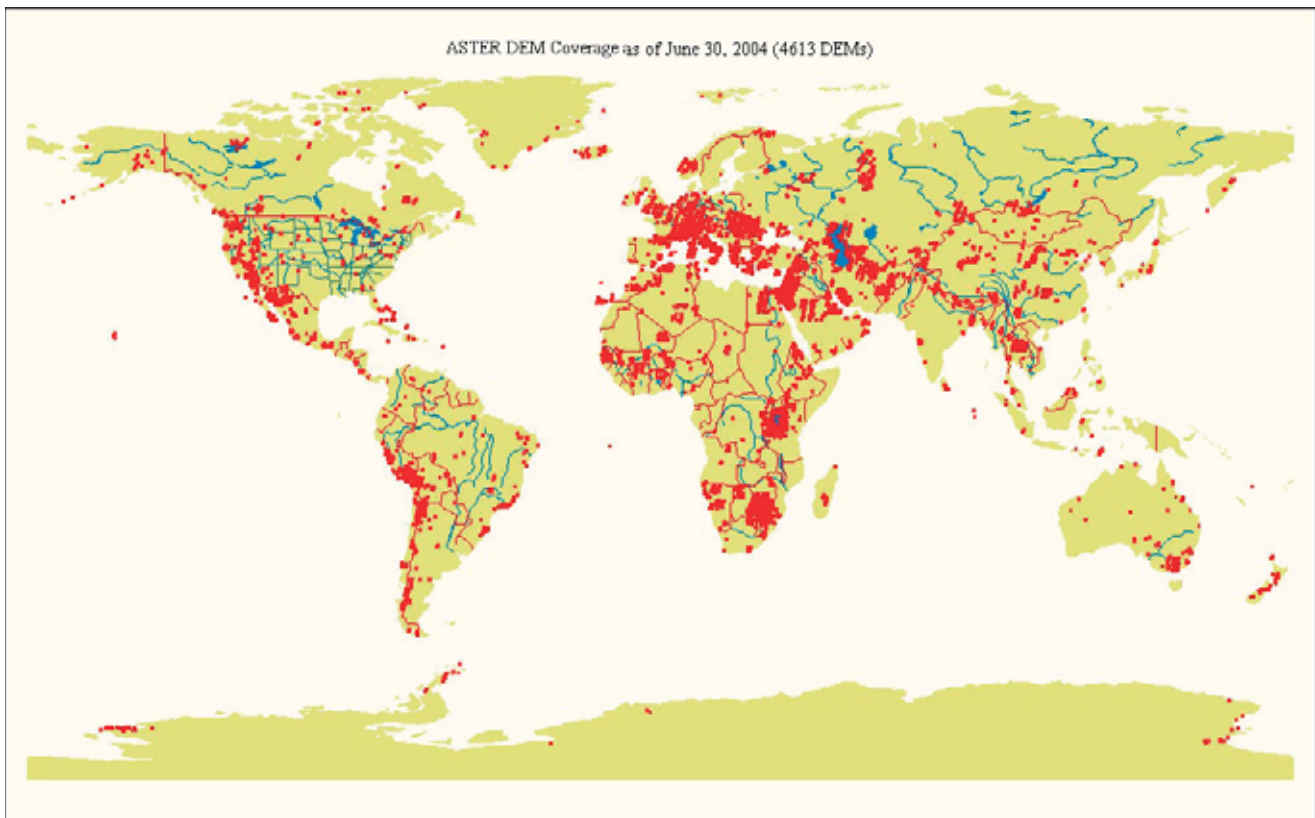


Figure 1. ASTER DEM coverage as of June 2004. Source: http://edcdaac.usgs.gov/aster/dem_map.asp

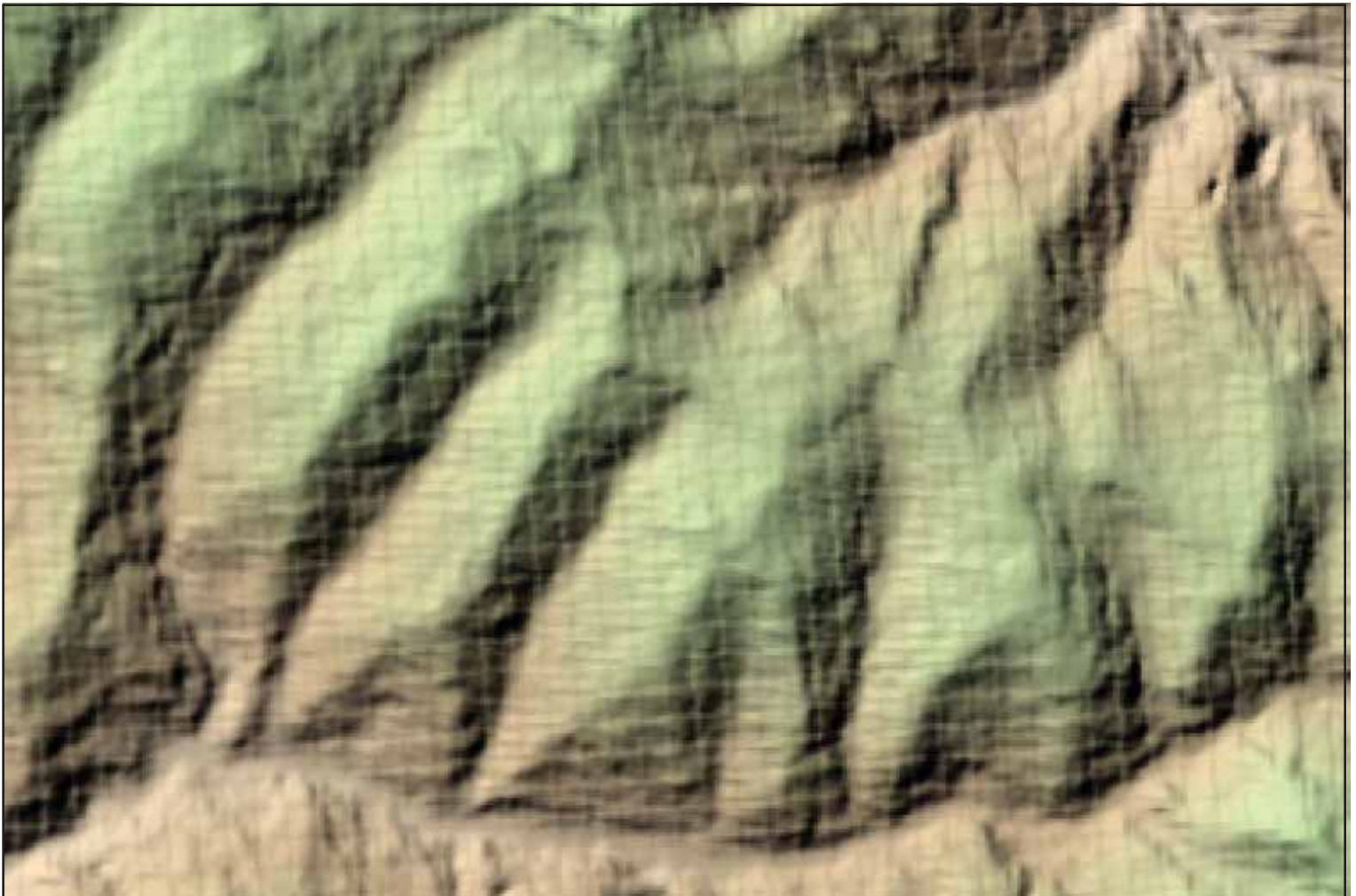


Figure 2. Shaded relief image of ASTER DEM displaying systematic patterning on the surface. scale 1:50,000.

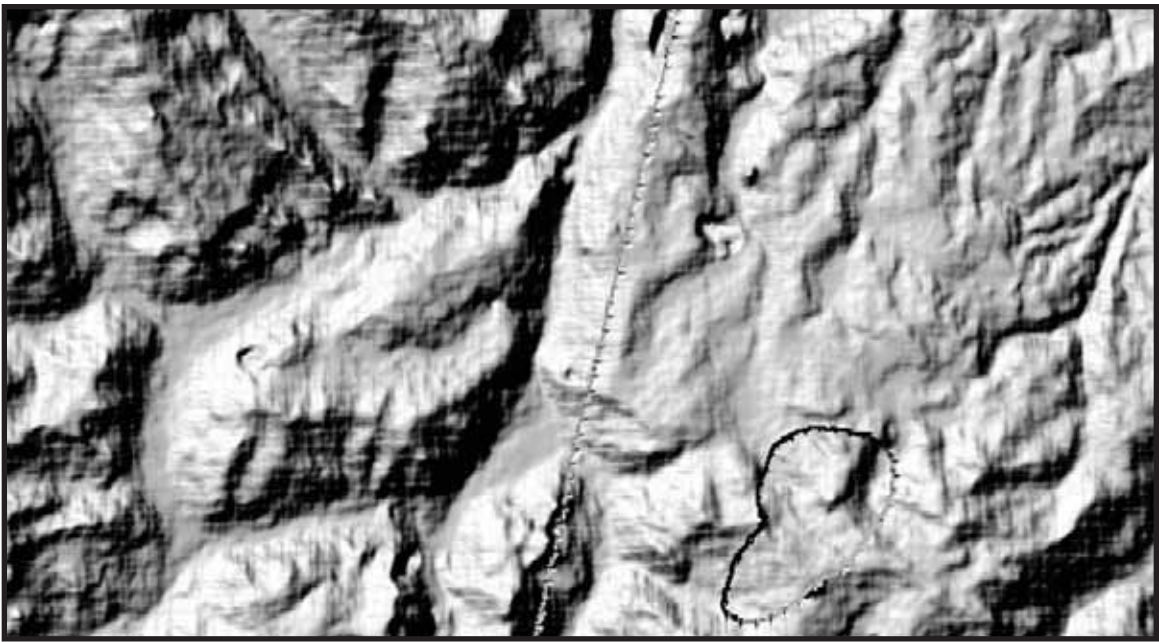


Figure 3. Seams quilted pattern on two merged ASTER DEM, 1:100,000



Figure 4a Terracing on Russian DEM

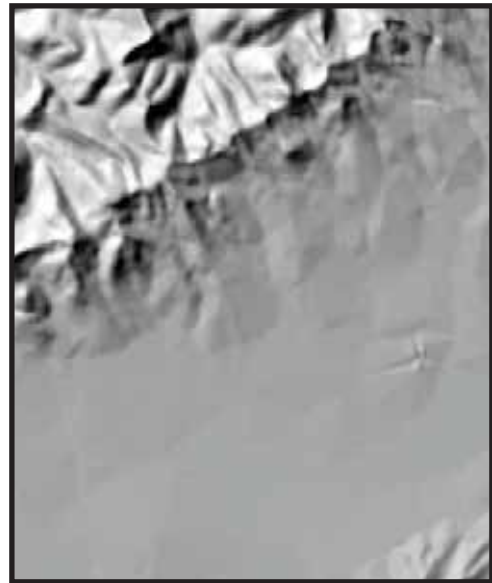


Figure 4b TIN artefacts on Russian DEM

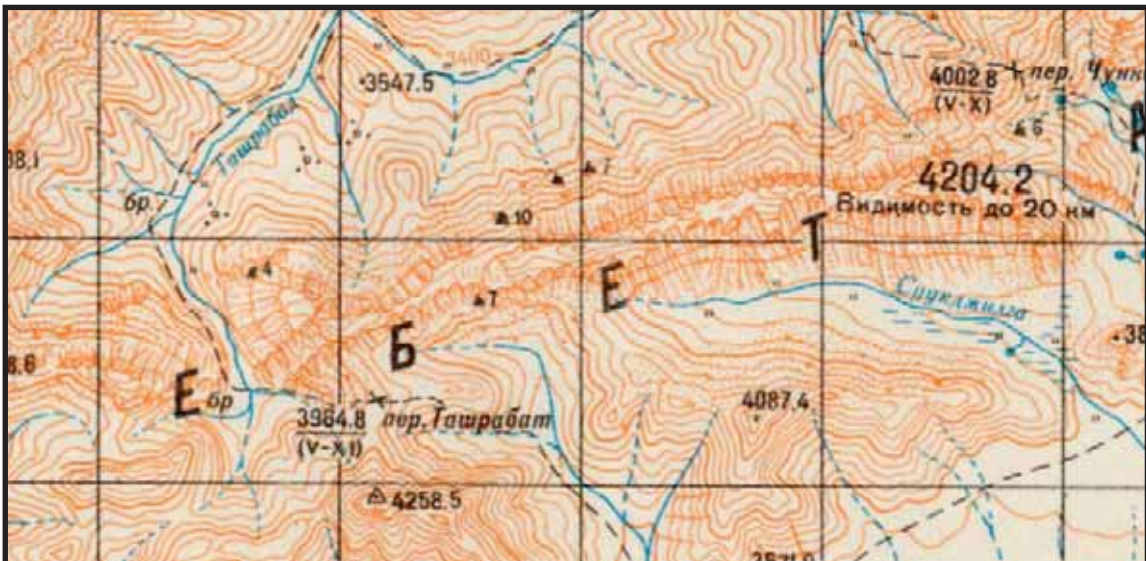


Figure 5 Scanned 1:100,000 Russian topo map of the Tash rabat area showing cliff drawings.

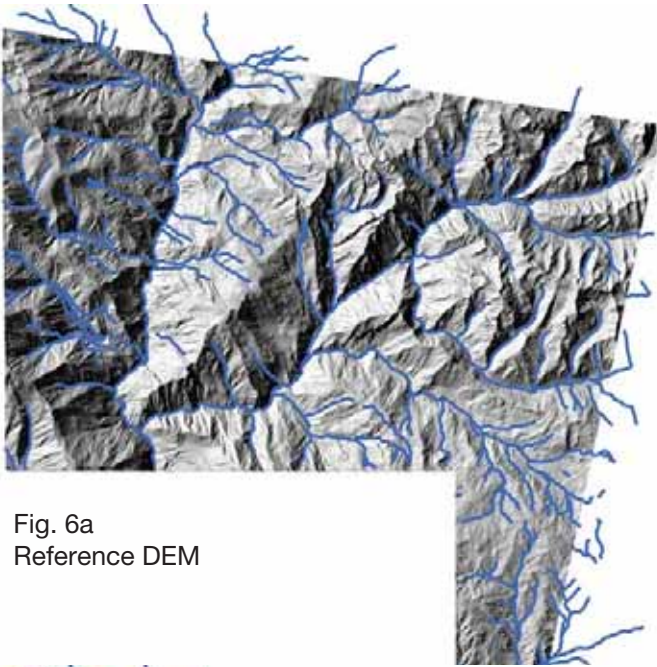


Fig. 6a
Reference DEM

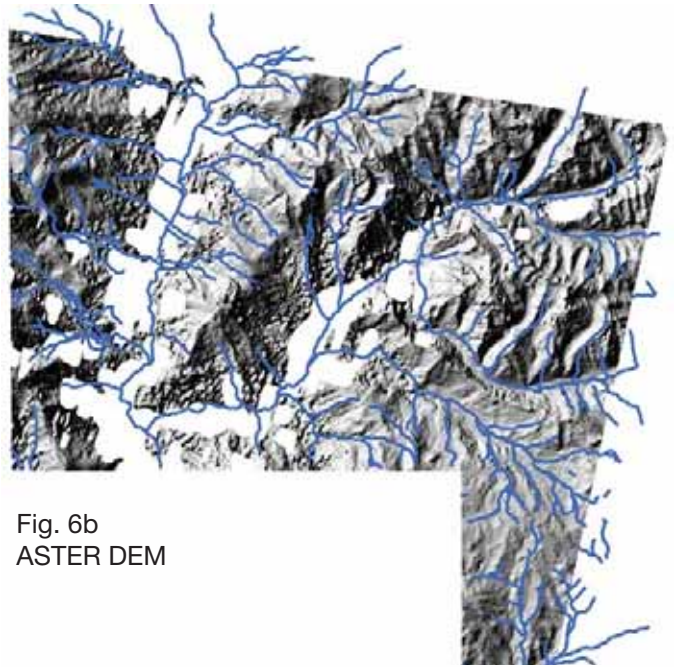


Fig. 6b
ASTER DEM

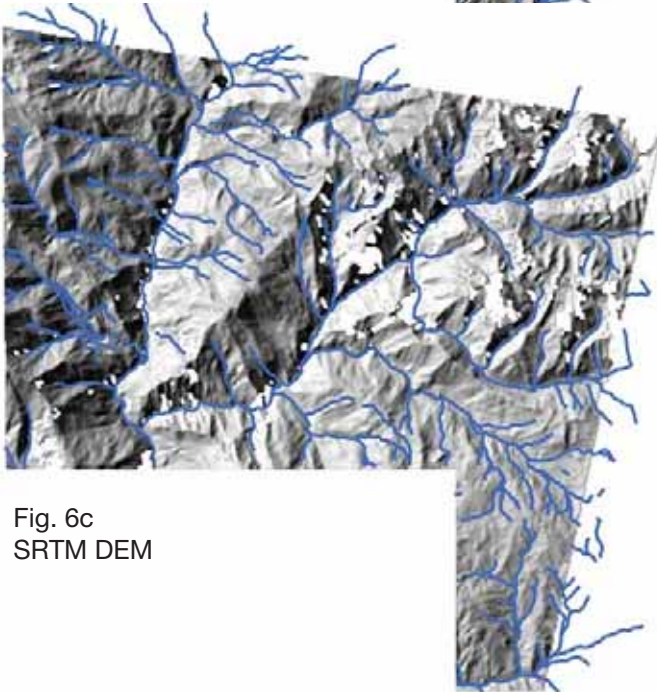


Fig. 6c
SRTM DEM

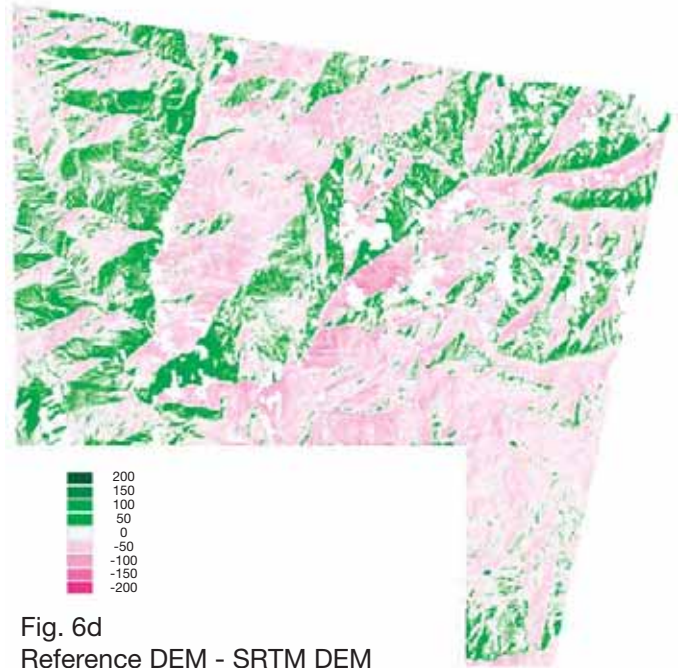


Fig. 6d
Reference DEM - SRTM DEM

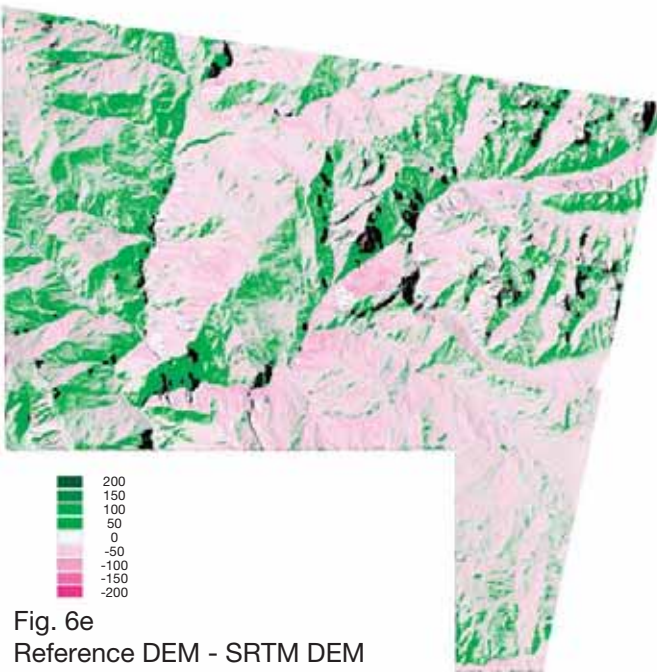


Fig. 6e
Reference DEM - SRTM DEM
with shading

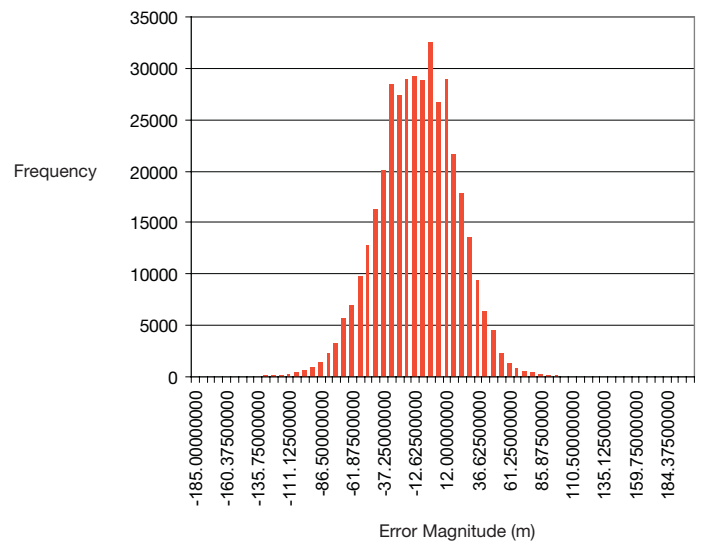
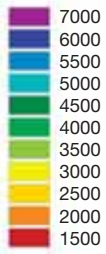
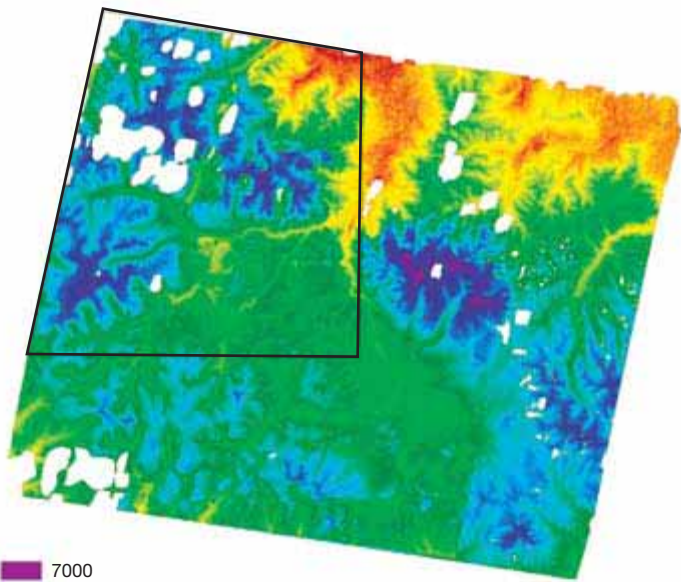
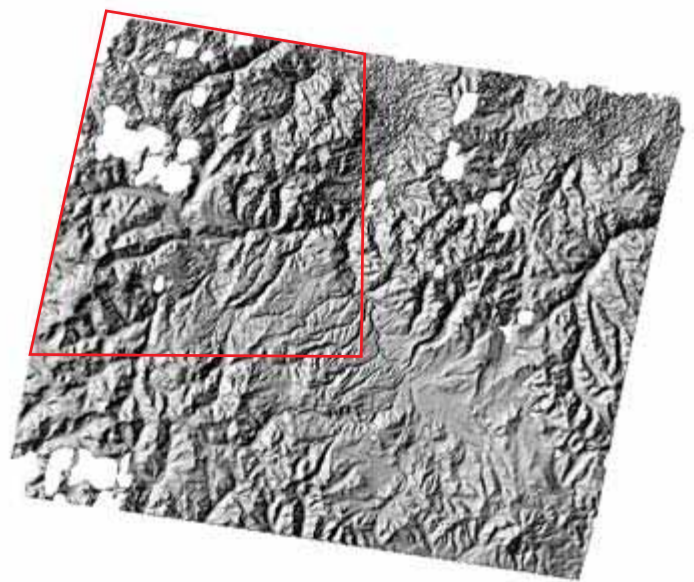


Fig. 6f. Histogram of error image



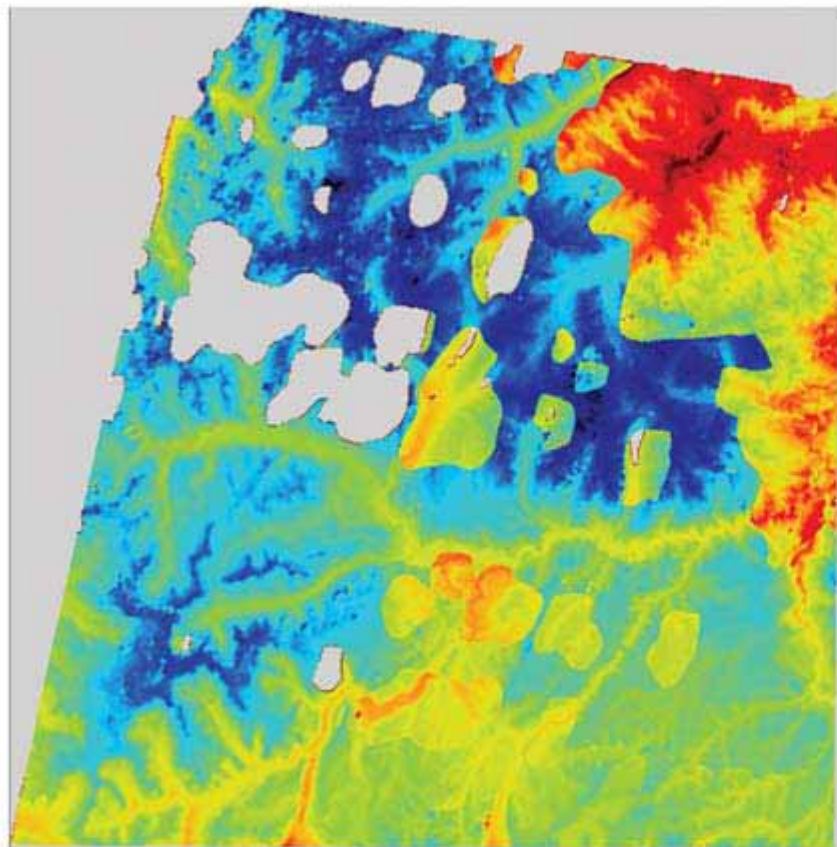
0 ~20 km

Fig. 7a Elevations of merged ASTER DEMs



0 ~20 km

Fig. 7b Shaded Relief of merged ASTER DEMs



0 ~20 km

Fig. 7c Distribution and magnitude of errors between reference DEM and ASTER composite DEM

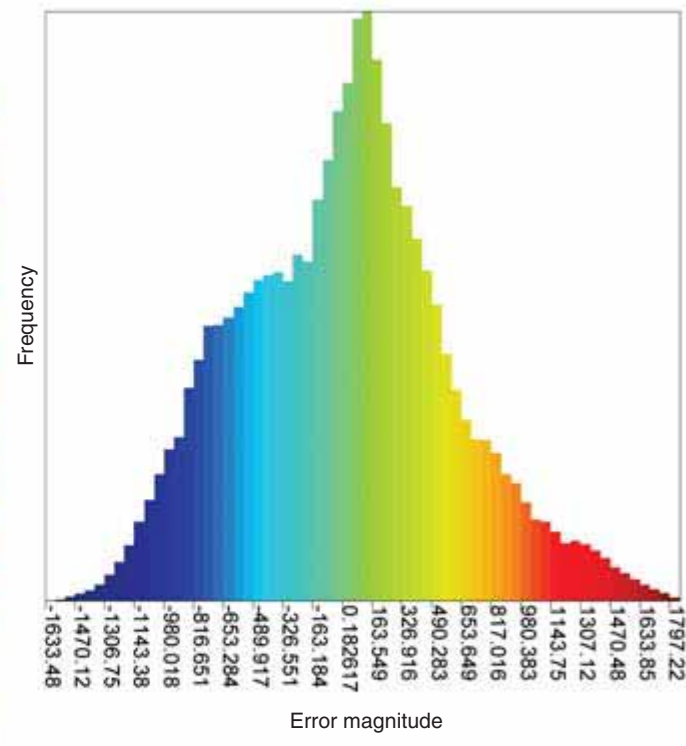


Fig. 8a Hypsometric tinting of SRTM DEM

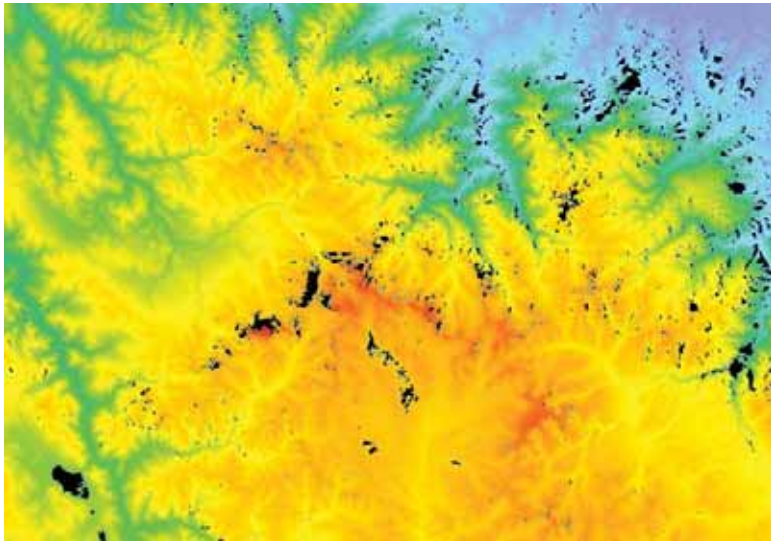


Fig. 8b Hypsometric tinting of SRTM DEM

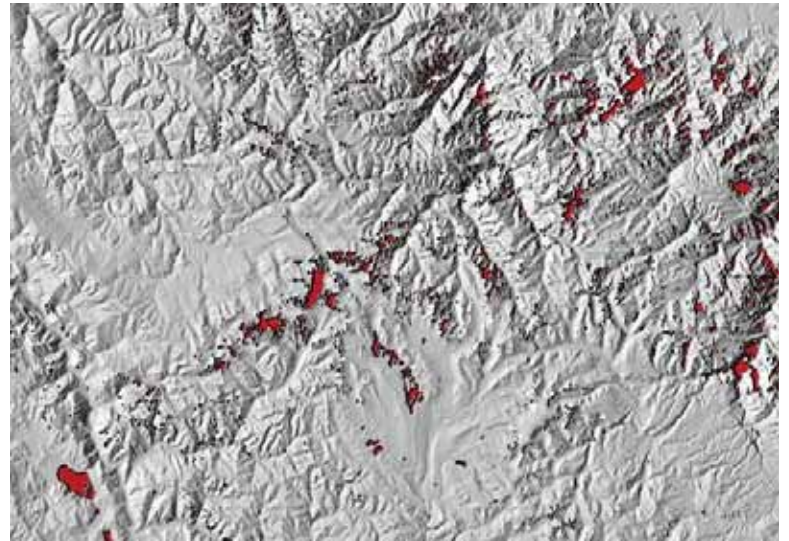


Fig. 8c Shaded relief of SRTM30 DEM

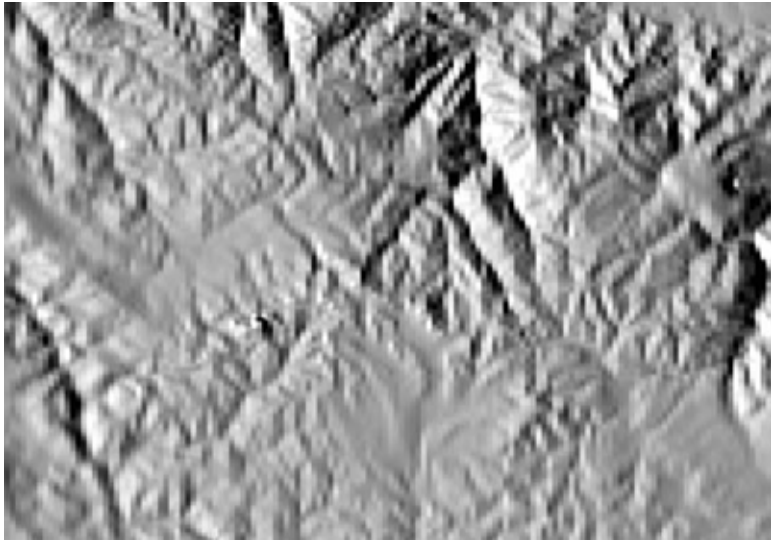


Fig. 8d Shaded relief of patched and filtered SRTM DEM

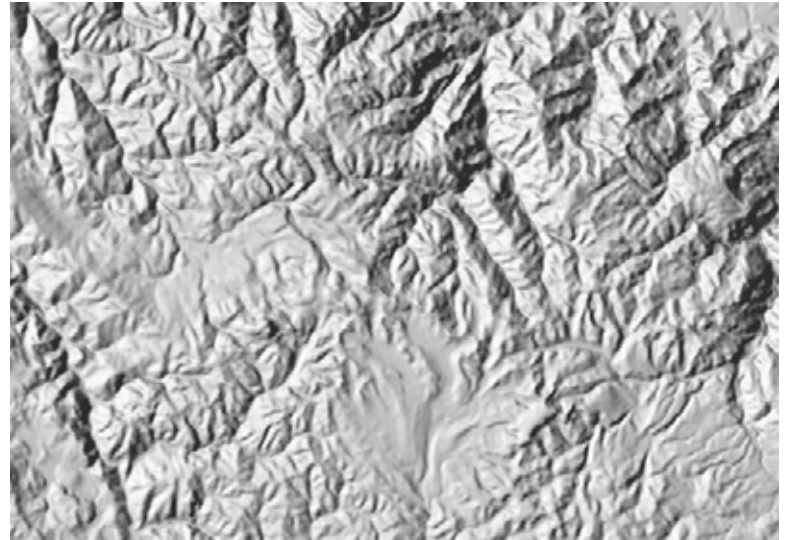


Fig. 8e Reference DEM from Peruvian IGN 1:100,000 topo map (left) and CIAT patched SRTM (right)

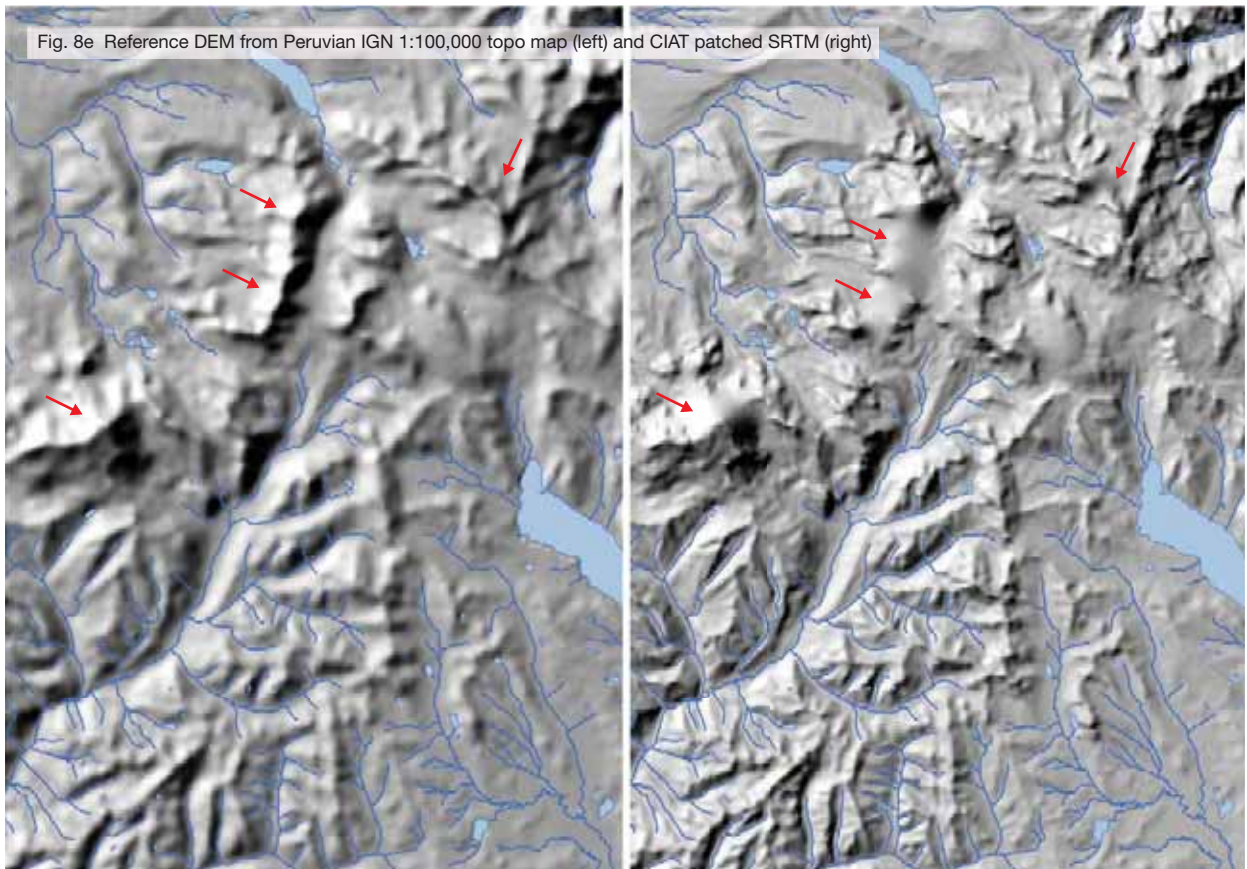


Fig. 9a Hypsometric tinting of ASTER DEM

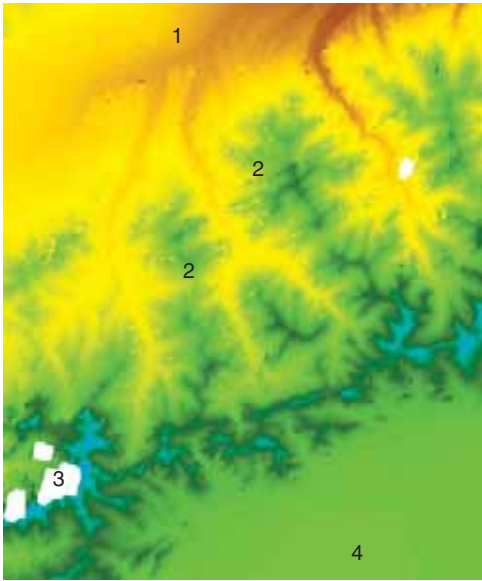


Fig. 9b Orthorectified ASTER VNIR image



Fig. 9c Finished base combining 9e & 9b

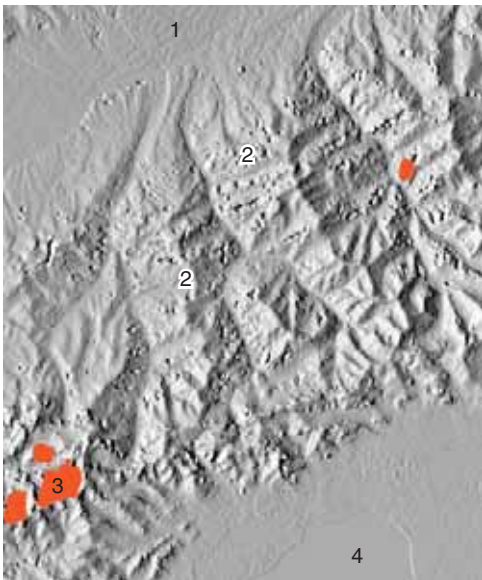


Fig. 9d Shaded relief of ASTER DEM

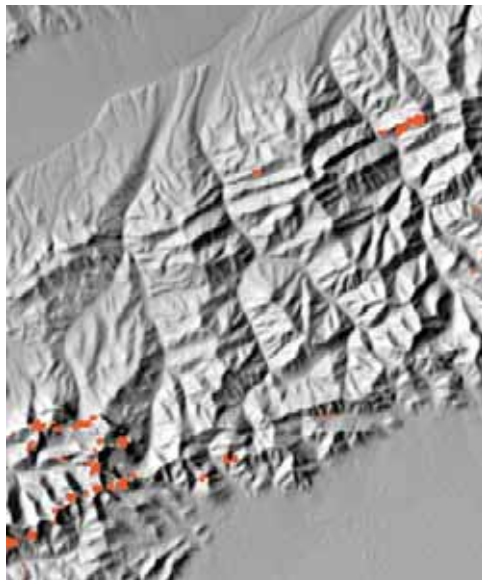


Fig. 9e Shaded relief of 90m SRTM DEM

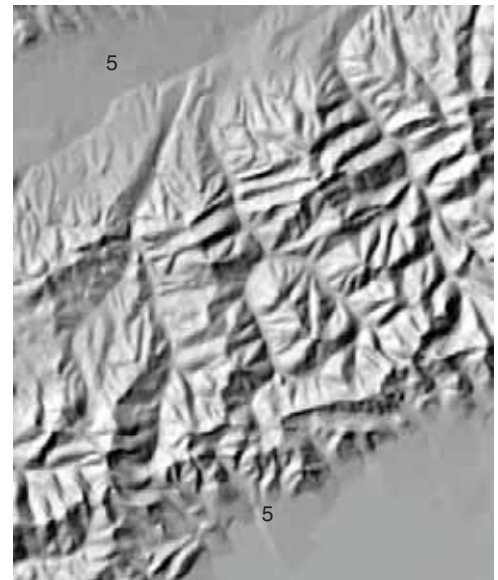


Fig. 9f Shaded relief of 90m Russian topo DEM

all images ~ 1:400,000

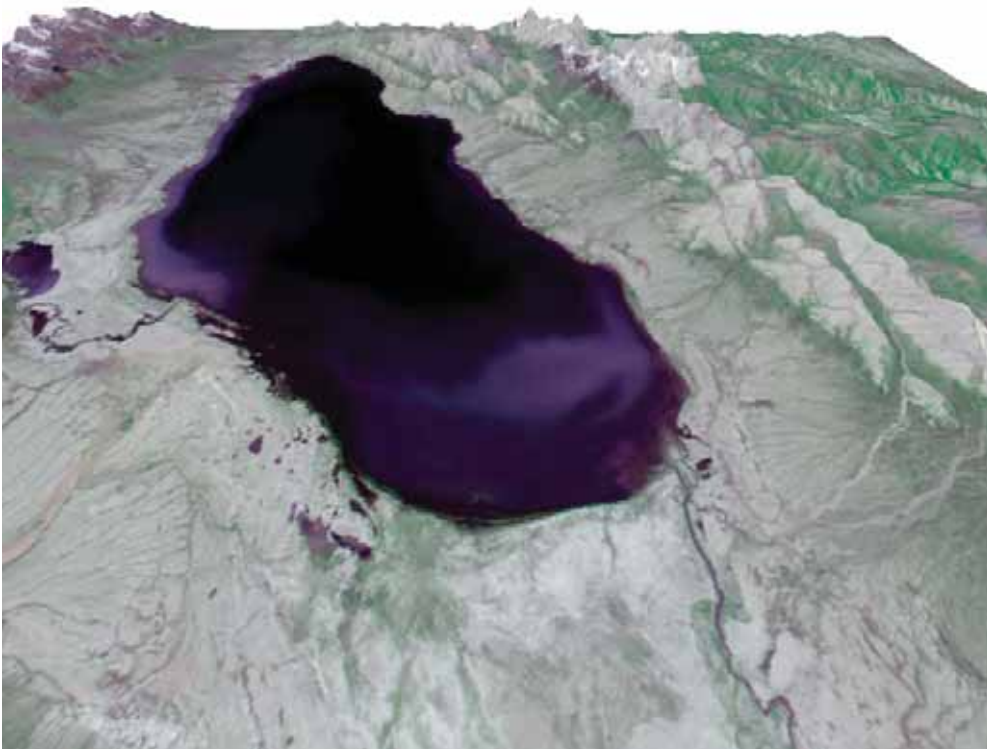


Fig. 9g Vue of Chatyr Kul from the north-east. ASTER VNIR image draped on ASTER DEM

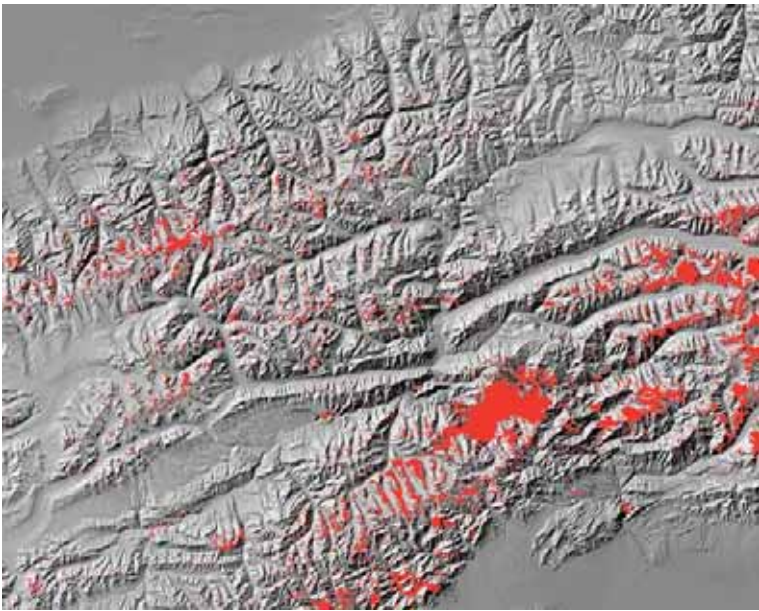


Fig 10a SRTM 90m shaded relief with data voids in red.

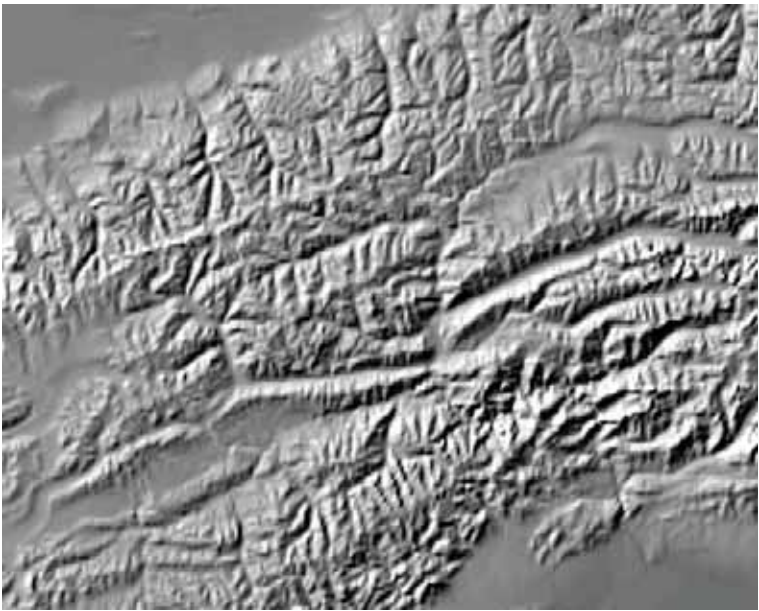


Fig 10b SRTM30 shaded relief.

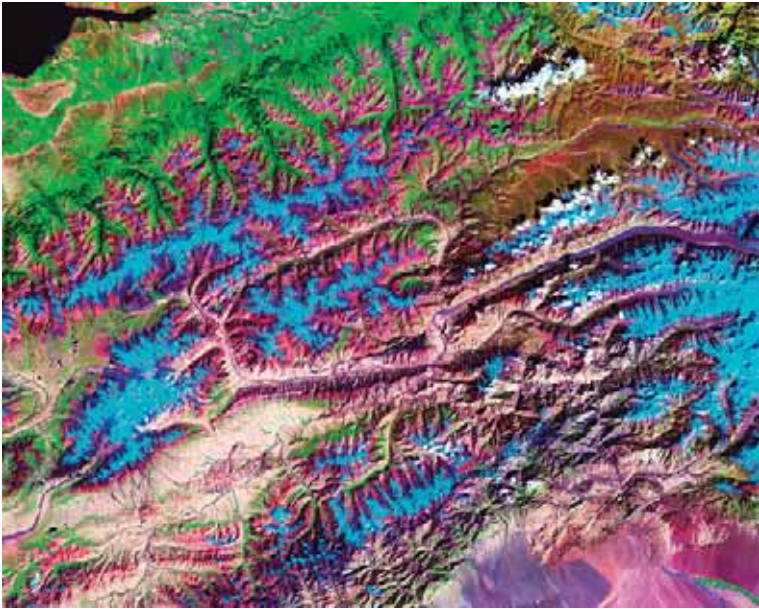


Fig 10c Geocover 1990 Landsat mosaic, note the prominent clouds.

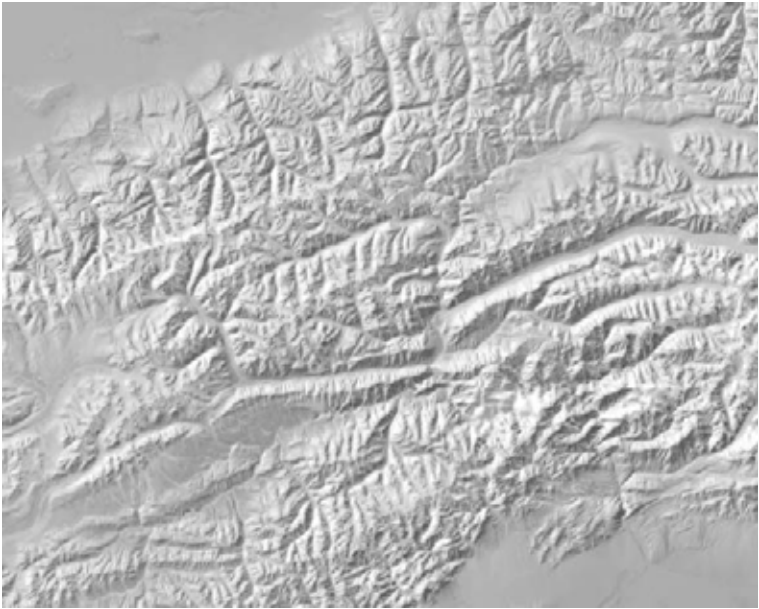


Fig 10d patched SRTM 90 shaded relief.



Fig. 10e finished base.



Fig. 10f finished map.

Fig .11a 3 arcsecond SRTM DEM with shaded relief, void areas shown in red

map scale: 1:200,000

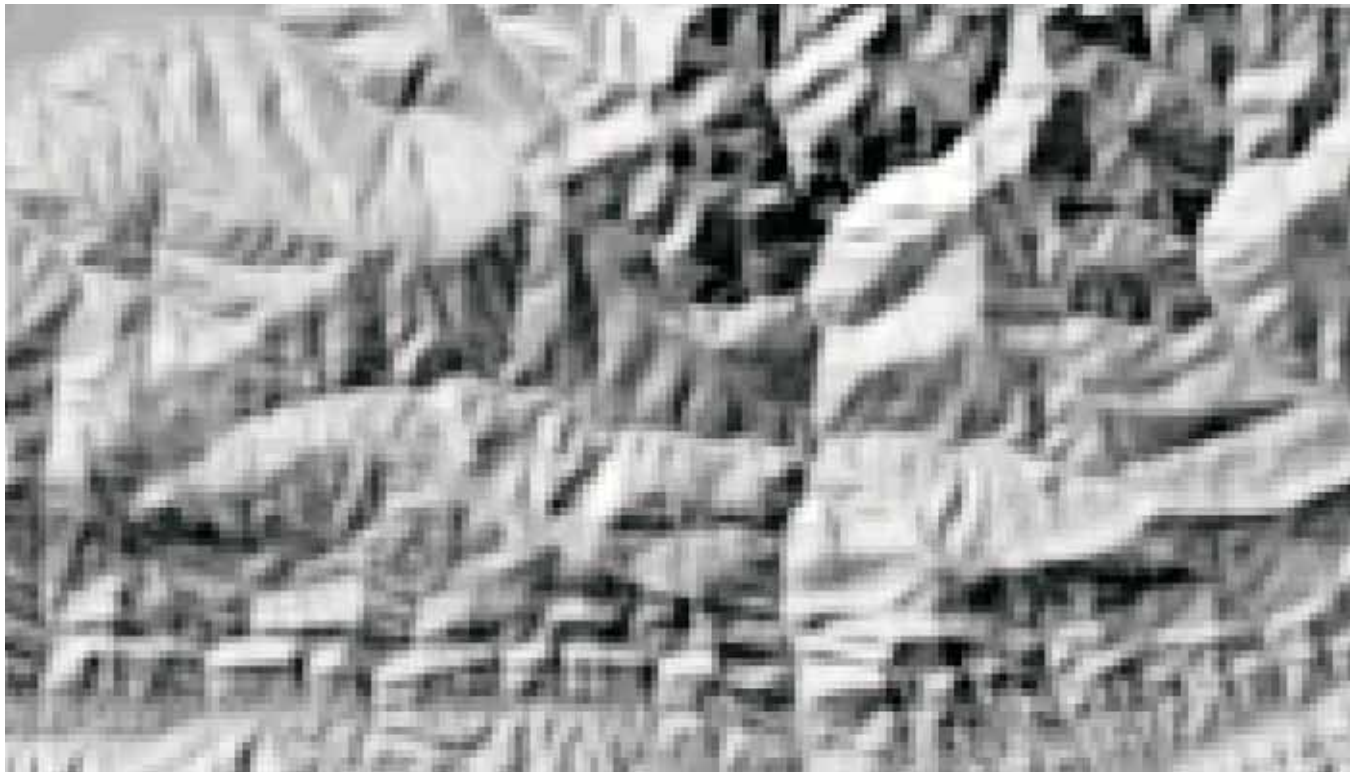
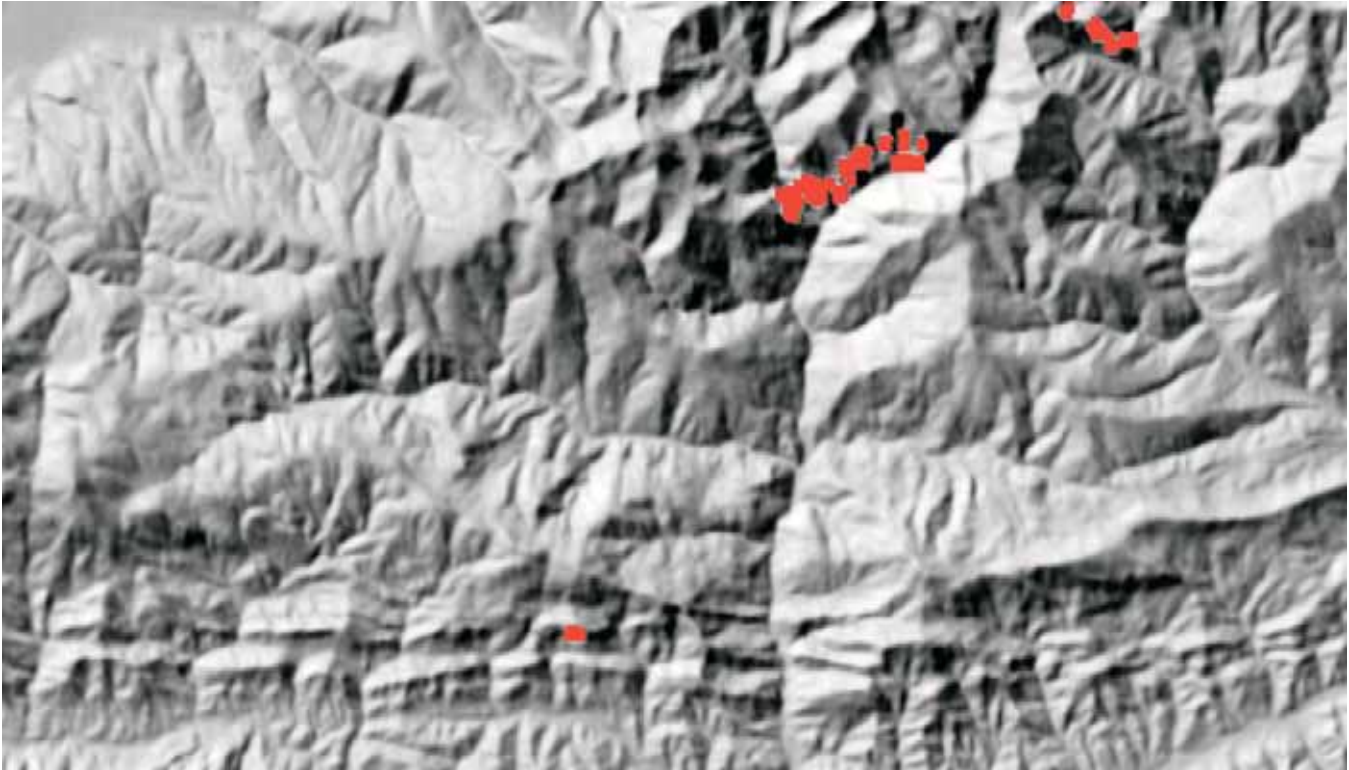


Fig .11b ICC 200m DEM with shaded relief.

map scale: 1:200,000

Fig .12a patched 3arcsecond SRTM DEM with shaded relief.

map scale: 1:200,000

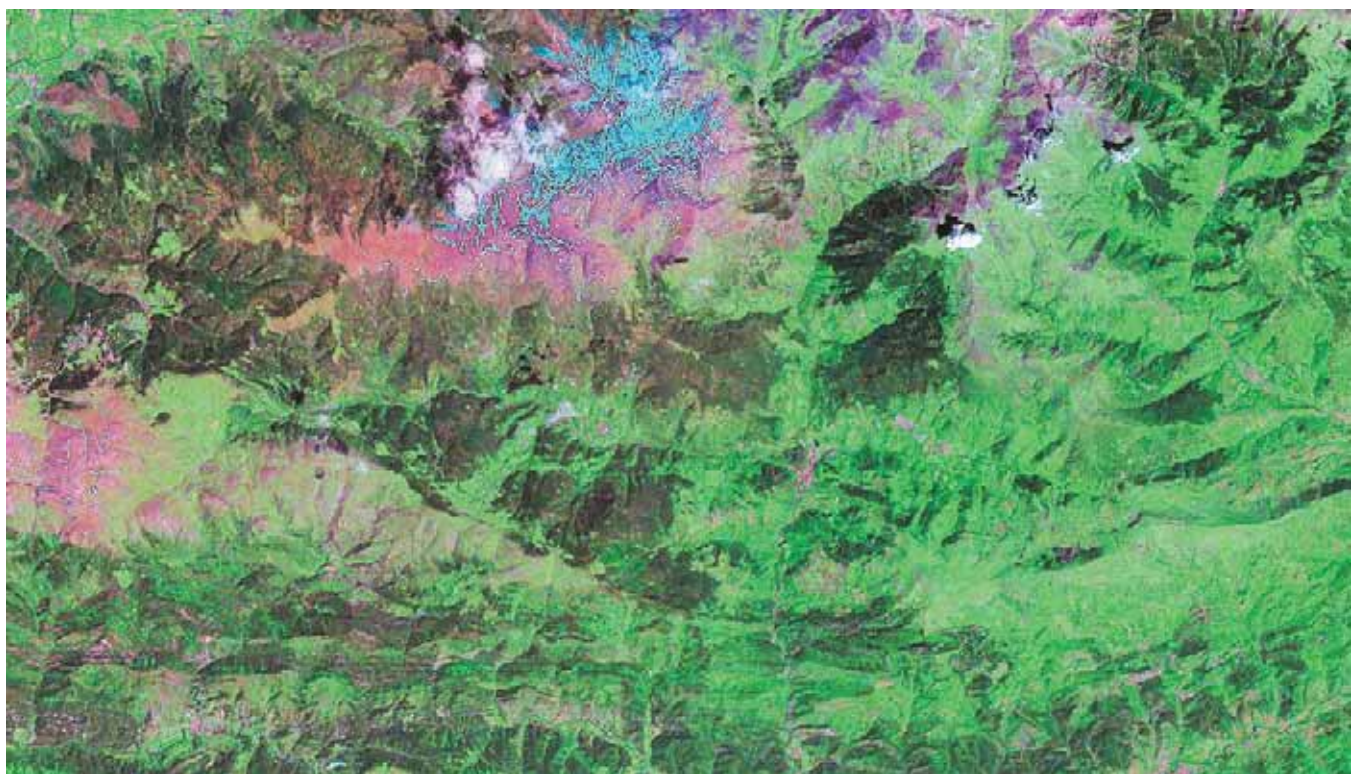
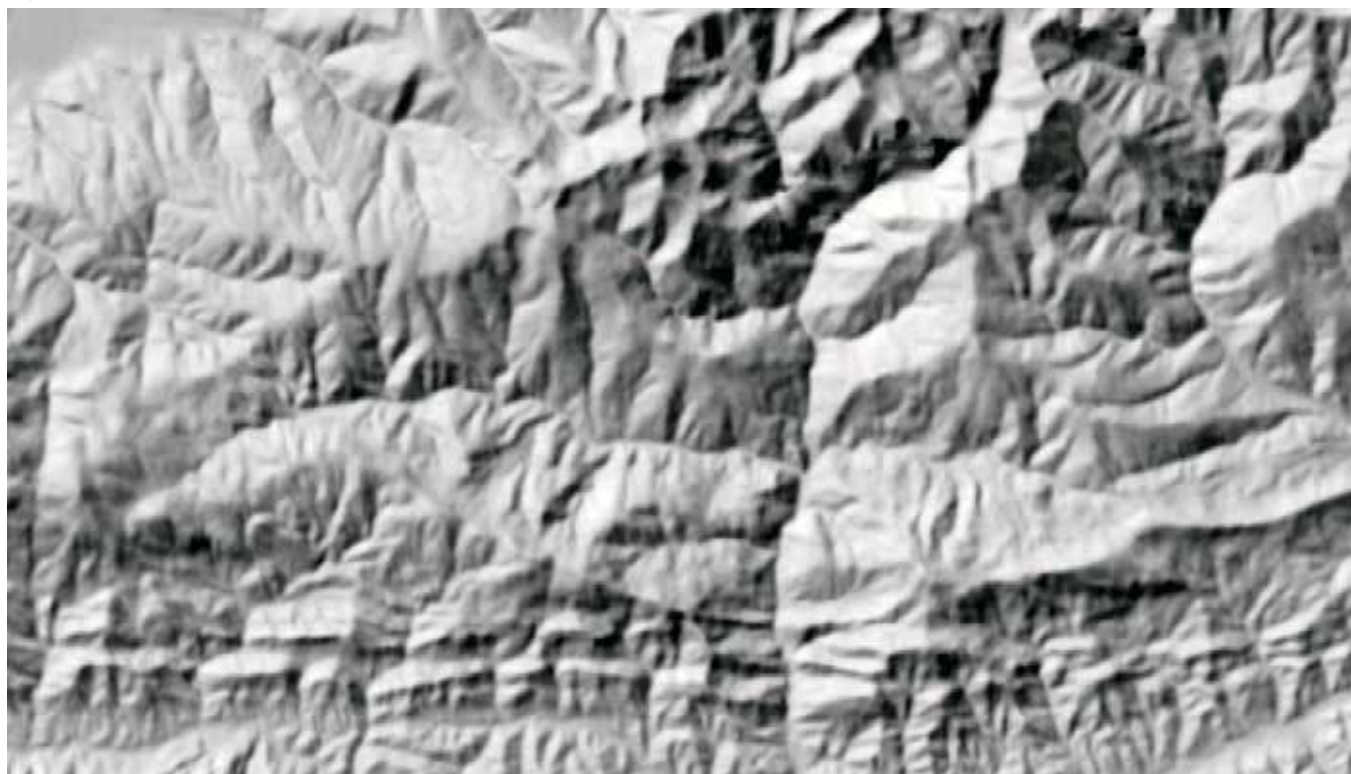


Fig .12b 14.5m pan sharpened Geocover mosaic.

map scale: 1:200,000

Fig .13a final image base combining 90m SRTM shaded relief and 2000 geocover mosaic.

map scale: 1:200,000

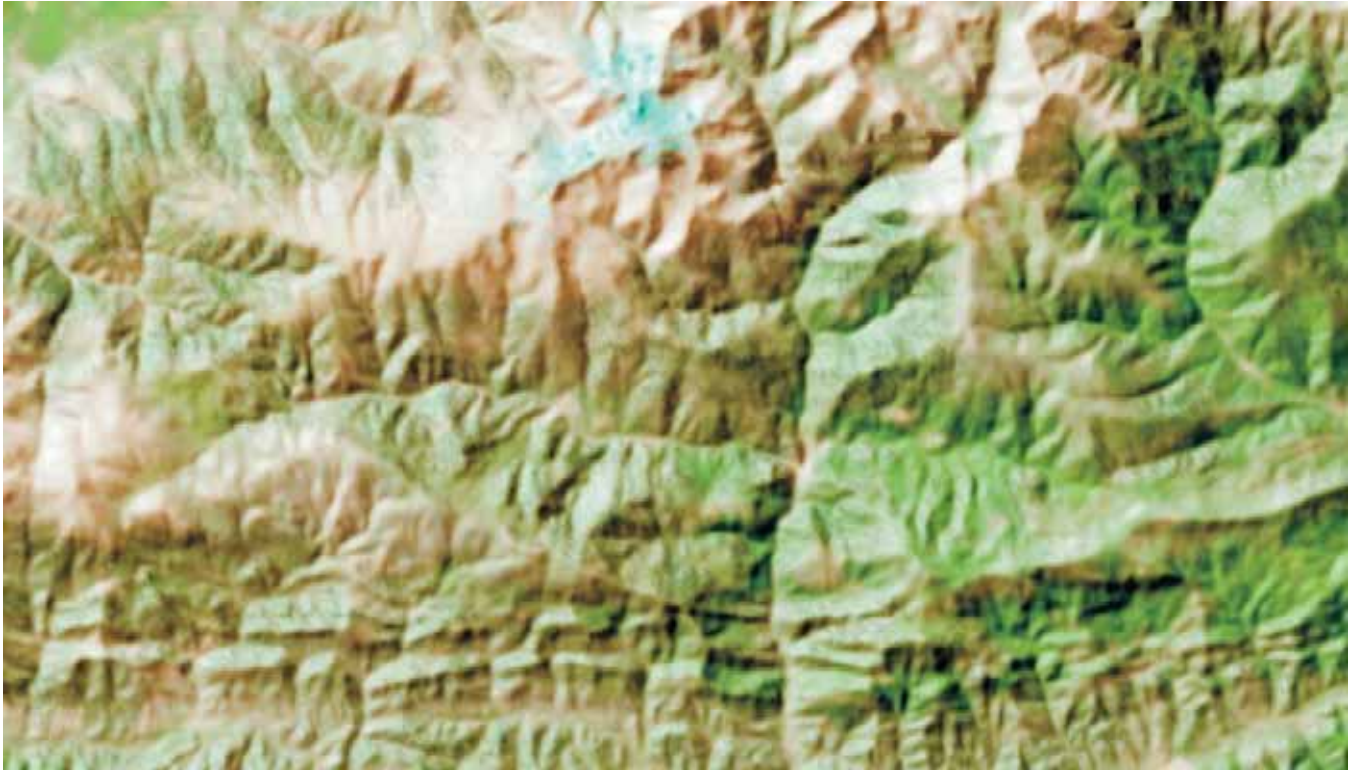


Fig .13b residual errors between ICC DEM and SRTM 3 arcsecond DEM

map scale: ~1:670,000

